Technological challenges on the road toward transparent networking

Stelios Sygletos,[1,*] Ioannis Tomkos,[2] and Juerg Leuthold[1]

[1]*Institute of High-Frequency and Quantum Electronics (IHQ), University of Karlsruhe, D-7613, Germany*
[2]*Athens Information Technology Center, 19.5 Km Markopoulou Avenue, 190 02 Peania, Athens, Greece*
**Corresponding author: s.sygletos@ihq.uni-karlsruhe.de*

Received October 23, 2007; revised January 22, 2008; accepted February 1, 2008; published March 21, 2008 (Doc. ID 88956)

The sustainable growth of high-bandwidth services and on-demand applications has introduced new challenges to next-generation networks in terms of capacity, configurability, and resiliency. Significant networking advancements need to be achieved with architectures and technologies that are scalable with respect to cost, size, and power requirements, while they should be capable of handling high traffic volumes and dynamically changing connection patterns. Transparent networking has the potential to meet those requirements and offer significant benefits in terms of performance and cost. We present the key enabling technologies, review the state-of-the-art achievements, and discuss the new opportunities that optical transparency has and will introduce.

OCIS codes: 060.1155, 060.1660, 060.2330, 060.2360, 060.4251, 060.4510.

1. Introduction

Transparent network concepts have gained significant attention in the past decade. In transparent networks, signals are transported end-to-end without being converted to the electrical domain along their path. This is in contrast to opaque networks, where optoelectronic regeneration is performed at every node.

The basic motivation for transparent networking was the realization that a significant portion of the network cost is in equipment needed to convert signals from the electrical to the optical domain. At the same time, traffic studies on the U.S. network topology demonstrated that the percentage of through traffic at each node ranges between 60% and 70% [1,2]. Therefore, the switching or routing capacity can be significantly reduced if those express channels bypass the electrical switches–routers right in the optical domain. This leads to significant capital expenditure (CAPEX) savings as a large number of expensive optoelectronic [optical-electrical-optical (OEO)] transponders are replaced by simple optical switches. This trend also provides savings in power and footprint, since the OEO converters are the main consumers of electrical power in the network and account for a big fraction of the overall footprint of the equipment. Furthermore, optical switches can deal with significantly higher capacities (~1 Tbits/s) than normal IP routers; therefore it is better to handle transit traffic in the optical layer, rather than switching it electronically. A transparent network is largely indifferent to the protocol, modulation format, and bit-rate characteristics of the propagated signals. This property enhances the upgradability of the networking infrastructure to accommodate increased bit rates associated with higher bandwidth requirements and new traffic types related to new services and applications. Optical transparency does not necessarily mean dynamic optical switching. Using static optical add–drop multiplexers (OADMs) transparent ring networks have been commercially available for metro applications since several years ago [3]. However, through the use of reconfigurable OADMs and optical cross-connects (OXCs) this feature can be advantageously associated to enable new revenue-generating services such as on-demand high-bandwidth provisioning, protection, and restoration.

Several shades of transparency may be envisioned spanning the spectrum of *strict transparency* to some subset, such as protocol, format, bit rate, or amplitude transparency. In a strictly transparent network the signals are transmitted optically from a source to any destination on any wavelength up to a predesigned maximum bit rate,

regardless of the bit rate, the protocol, or the framing structure used. Such transparencies are lost when the network is equipped with OEO transponders that use standardized digital frames such as a synchronous digital hierarchy (SDH) and synchronous optical networking (SONET) or an optical transport network (OTN) to perform switching, forward error correction (FEC), and other intelligent control functions in the electrical domain. On the other hand, all-optical devices do not necessarily provide *strict transparency*.

Another term needs clarification—the term "all optical." Generally, a device is labeled all optical if it performs an operation in the optical domain that traditionally would be expected to be performed in the electrical domain. However, in practice (though not in this paper) the term is often used when actually speaking about transparent networks. All-optical devices do not necessarily provide *strict transparency.* In fact, most all-optical devices provide transparency to a certain degree [4,5]. Typically they provide full protocol transparency and bit-rate transparency within certain limits. Yet they are usually not amplitude transparent; instead they may be regenerative.

Real catalysts behind the evolution of transparent networking were a number of technical breakthroughs that took place in optical communication research and accelerated the implementation of integrated transmission and switching functionalities in the physical layer. The scope of this paper is to present those new technologies that led to the development of high-capacity networking infrastructures able to accommodate, in a cost-efficient way, the rapidly growing size of Internet traffic demands over terrestrial and ultra-long-haul distances.

In Section 2 a historical review is presented on the milestones that boosted the evolution of optical communication systems from fully opaque single-channel point-to-point connections towards wavelength-division-multiplexing (WDM) transparent networks [6]. In Section 3 the technological challenges that this new concept has introduced on the transmission, switching, and control planes of the network are discussed. Finally, in Section 4 the key enabling technologies are presented in detail and the state-of-the-art progress in the field of dynamically reconfigurable networking based on cross-layer optimization is reviewed and the future potential advancements are analyzed.

2. Historical Evolution toward Transparent Optical Networks

The first optical transmission systems were deployed in the 1970s and were based on multimode fibers and light-emitting diodes (LEDs) or laser transmitters in the 0.8 and 1.3 μm bands, while their operating bit rate did not exceed 140 Mbits/s [6]. The dominant degradation factor was intermodal dispersion; therefore OEO regenerators were required every few kilometers ($\sim$10 km) to refresh the propagated waveform. However, these regenerative subsystems were quite expensive and one of the main design challenges that engineers had to face at that time was how to reduce their number in a transmission link.

The deployment of single-mode fibers in the next-generation transmission systems, in the mid 1980s [7,8], eliminated the distortions due to intermodal dispersion and enabled much higher bit rates of several hundred megabits per second. Furthermore, the distance between regenerators was extended to 50 km. The operating wavelength of those systems was 1.3 μm and the prime limiting factor was the fiber loss. To enable even longer distances between the regenerators the researchers soon focused on the minimum loss window of 1.55 μm. However, at that wavelength band, chromatic dispersion appeared as the main degradation factor that could prevent any upgrade to higher bit rates. The development of dispersion-shifted and dispersion-compensating fiber enabled this problem to be overcome. Another improvement came from the development of single-mode laser sources such as distributed-feedback lasers (DFBs). Their narrow spectral width significantly reduced the penalty due to chromatic dispersion and allowed further increase in the bit rate ($\sim$1 Gbits/s).

The advent of Er-doped fiber amplifiers (EDFAs) introduced a major technological breakthrough, which spurred the development of a new generation of WDM transmission systems. Their most significant advantage was the simultaneous amplification of many wavelength channels of copropagating signals in the fiber [9,10]. This dramatically decreased the cost of the long-haul systems since a cheap EDFA could replace a whole array of expensive optoelectronic regenerators at each repeater point. Yet, with

the advent of EDFAs, new impairments arose, such as the accumulated amplified spontaneous emission (ASE) noise, the nonflat gain spectrum of the EDFAs, fiber nonlinearities, and polarization effects. To mitigate those effects, new technologies were introduced, such as Raman amplifiers, novel modulation formats, advanced dispersion management schemes, FEC, gain equalizing filters, etc. These enabled one to tremendously expand the distance between the regenerators up to several thousands of kilometers as well as to increase the transmitted capacity up to several terabits per second [11–18]. The advances that took place in the WDM long-haul technology over those 10 years offered significant CAPEX savings. The majority of optical systems in use today were installed during the period from 1999 to 2001, and such systems are referred to as the second generation. Such systems support simultaneous transport of 60–80 channels in the backbone network with a maximum of 10 Gbits/s per channel via one optical fiber. These networks, also called opaque networks, were typically OEO-based, with all traffic routed through a node being converted to the electronic domain, regardless of whether or not the traffic is destined for that node. Typically, the OEO converters are transponders, which are a combination of a transmitter–receiver card that has a short reach interface on the client side and a WDM-compatible signal on the network side. Current WDM systems have usually been equipped with transponders that employ the SONET–SDH format and provide both signal regeneration functionality as well as monitoring of the optical channels. The transmission part of the network is used as a server layer for the connections of the SDH cross-connects, the asynchronous transfer mode (ATM) switches, and the IP routers. A typical opaque network node is depicted in Fig. 1(a). Most of the traffic of service networks is multiplexed and groomed by SONET–SDH and then transported by optical channels.

The next evolutionary step was toward a transparent switching node. This was introduced with the emergence of OADMs and wavelength-based OXCs [Fig. 1(b)] that allowed for optical bypassing of nodes [19,20] and provided, under network control, the ability to drop and add wavelengths (OADM) or more generally to connect any input wavelength from an input fiber to any one of the output fibers (OXC). In addition, they enabled power leveling, possibly wavelength monitoring, and connection verification.

While first transparent network deployments are basically transparent point-to-point links with OADMs at intermediate nodes, the trend is toward so-called islands of transparency and potentially toward fully meshed transparent networks with OXCs in the near future [21]. A critical parameter in this case that determines the cost-effectiveness of such systems is the optical reach, which is the distance an optical signal can travel before needing to be regenerated [22]. Although a longer optical reach leads to a reduction of the number of expensive OEO regenerators, these benefits are expected to be counterbalanced by the extra cost of the high-performance devices such as amplifiers and transponders [23]. The optimal optical reach can be identified through network dimensioning analysis and is influenced by parameters such as the network topology, the traffic demands, the cost, and the physical performance of the network elements [24].

Furthermore, transparent networks are evolving from static to dynamically reconfigurable and flexible infrastructures with fully tunable characteristics. Network reconfigurability has been identified as a vital solution to support traffic pattern changes. The main benefit that these networks are expected to offer to operators and service providers is the ability to efficiently utilize and also extend their resources according to the offered services without affecting the existing traffic, which is

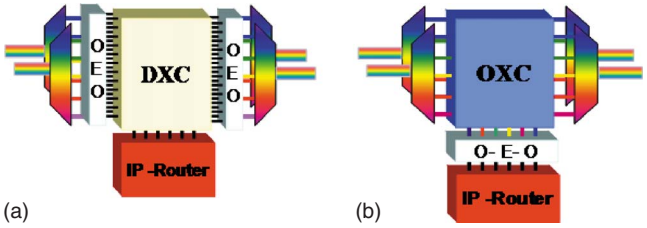

Fig. 1. Node architectures with (a) digital cross-connect (DXC) and (b) all-optical cross-connect (OXC).

expected to result in simplified network planning and provisioning and to significantly reduce the operational cost. This need is currently followed by major equipment and system vendors providing reconfigurable node solutions [e.g., reconfigurable OADMs (ROADMs)] that are able to support multiple channels and data rates up to 40 Gbits/s.

Transparent networks with the aforementioned features have already been developed into commercially available products [25]. A notable example is the Verizon business network deployment, which consists of several regional systems that are connected via ROADMs–OXCs and extend over the entire geographical area of the continental United States [26]. This network uses the LambdaXtreme transport system platform, which employees distributed and discrete Raman amplifiers to achieve very high-capacity and long reach [27]. Specifically, it uses a single transmission band, from 1554 to 1608 nm and it enables a capacity of 128×10 Gbits/s for 4000 km and 64×40 Gbits/s for at least 2200 km. It also includes automatic power optimization, dynamic gain equalization, wavelength blockers for use at ROADMs–OXCs nodes, and a high-capacity optical supervisory channel. This technology represents significant innovations in system architecture, transmission and amplifier design, software control, and network design tools. It is uniquely suited to address the increasing capacity needs of network operators and realize the vision of optical transparency in core optical and backbone networks.

3. Requirements and Challenges of Transparent Optical Networks

The realization of transparency, though highly desirable due to the expected cost and performance benefits, generates a new set of considerations and technical challenges in the switching, transmission, and control planes of the network.

As already mentioned the migration from point-to-point transmission links into elaborate networking topologies is facilitated with OADMs and OXCs. Ideally, these architectures should provide similar switching functionalities to those of the SONET–SDH layer, but with improved manageability and lower complexity and cost [28,29]. Apart from the bit rate and format transparency they should also be scalable and have the capability to drop any channel as well as to insert any other channel on any unused wavelength. In addition, nonblocking is required for the OXCs' connectivity. To achieve flexible path provisioning and network resilience, dynamic reconfigurability at millisecond time speeds should be provided without introducing any disruption on the existing traffic during the reconfiguration process [30,31]. In transparent networks the optical path is not confined between two consecutive nodes, but it might traverse a number of them. To maximize the transparent length of the connections it is important to ensure that the induced degradation on the quality of the propagated signal is minimized at each node. Therefore, a high ON–OFF ratio (>35 dB) is required between the output power levels at the on and off states of the switches to prevent the accumulation of cross talk [20]. Furthermore, low insertion losses are needed to avoid severe degradations on the optical signal-to-noise ratio (OSNR), while it is highly desirable that these losses are insensitive to the polarization state of the input signal [32]. In a long chain of amplifiers a change in the spectral loading introduced by adding or dropping in OADMs or switching in OXCs may cause gain tilt and severe transient effects as rapid variations of the amplifier input power level may cause unwanted sudden gain increase [33–36]. This problem is commonly overcome by using fast amplifiers to gain control as well as fast dynamic spectral equalization that can be provided by corresponding elements at the OADM–OXC nodes, which are commonly called dynamic gain–dynamic spectral equalizers (DGEs–DSEs). In general, these elements can have a very important role in transparent optical networks for mitigating signal power divergence between the various wavelength channels. This effect is attributed to several factors, such as the spectral dependence of the component-induced insertion loss, the amplifier gain spectrum variations, nonideal multiplexer (MUX)–demultiplexer (DEMUX) filters, and polarization-dependent losses, as well as fiber loss variations along the wavelength plan [37]. Another critical issue is the design of the filter shape. The optical switching nodes incorporate some filtering to isolate and route individual wavelength channels. If several nodes are cascaded, the optical path of a WDM wavelength channel experiences spectral narrowing due to the combined effect of all the cascaded filters. The penalty introduced by this

phenomenon strongly depends on the spectral characteristics of the transmitted signal and therefore the modulation format used. The effect is emphasized further by any filter misalignments present in the system.

Transparent bypassing of the OEO regenerated stages results in accumulation of the signal impairments that limit the system reach and the overall network performance. A variety of quality-degrading phenomena such as ASE noise, chromatic dispersion (CD), polarization mode dispersion (PMD), and nonlinear (NL) effects introduce different types of signal distortions. For example, there are distortions of an almost deterministic type related only to the single channel's pulse stream and that are introduced by the CD, the intrachannel nonlinearities, or the optical filtering. The other category includes phenomena such ASE noise, four-wave mixing (FWM) and cross-phase modulation (XPM), and cross talk that can be considered as small perturbations on the signal waveform. The limitations by noise, CD, and PMD become even more critical with increasing data rates, i.e., going from 10 to 40 Gbits/s [37–39]. A way to extend the system reach is by employing a combination of advanced modulation formats [duobinary, differential phase-shift keying (DPSK), differential quaternary phase-shift keying (DQPSK), etc.] together with FEC coding and electrical and optical equalizers for PMD and CD [40,41]. These techniques are expected not only to allow for transparent bypassing and thus to reduce or eliminate a number of components associated with the network nodes but also to offer increased performance [37–41].

Upgradeability to higher bit rates is a key requirement for the transparent network. Also, accommodation of both 10 and 40 Gbits/s in optical nodes definitely would be desirable. Yet operation at 40 Gbits/s is very challenging primarily for two reasons. First, because 40 Gbit/s networks require larger spectral bands than 10 Gbit/s networks, and, second, because most modulation formats that have been proposed initially for 40 Gbit/s systems have wider bandwidth requirements than the conventional non-return-to-zero (NRZ) modulation format usually used for 10 Gbit/s networks. Recent efforts to upgrade existing infrastructures to 40 Gbit/s are focused on a number of techniques such as using advanced modulation formats, some of which have narrower spectral bands and thus might be useful to upgrade existing 10–40 Gbit/s networks.

Dynamically reconfigurable networks bring the benefits of dynamic bandwidth allocation and efficient resource utilization; however, their window of operability can be significantly reduced due to the temporal variability of the transmission parameters. The copropagating channels have different histories and path lengths; thus, point-to-point optimization is not applicable anymore. New design strategies are required to accommodate the variety of the different conditions that are encountered in this heterogeneous environment. One option is to define the performance limits of the transparent network based on simple and constant design rules. In particular, some generic dispersion mapping could be implemented so as to enable the bridging of various distances of the optical paths with reasonable performance, while minimizing complexity. The traffic that requires support outside the framework must be regenerated so that it falls within the design rules. Such an approach has been demonstrated in [42], where it has been shown that by using simple CD management and power management an interesting quantity of Pan-European network traffic could be supported without regeneration. Another proposed solution is associated with the use of tunable (colorless) devices both at the transmitter–receiver end and the switching subsystems. Tunability will enable optimum network planning and simultaneous real-time reconfiguration according to the traffic pattern variations in the network and the resource availability in terms of wavelength channels, link bandwidth, switching ports, etc. Their dynamic behavior is expected to reduce the impact of the transmission impairments because the system can be reoptimized as the physical properties of the light paths change with time as the network is reconfigured. The colorless devices and subsystems include tunable transmitters and receivers (e.g., lasers and filter), dynamic gain equalizers, variable passband switching elements, and adaptive optical and electronic dispersion compensators [43–46]. A third approach that could be considered for future core networks, in addition to physical layer impairment management techniques, is the use of certain routing and wavelength assignment (RWA) algorithms that take into account the signal impairments and constrain the routing of wavelength channels according to the physical characteristics of the optical network paths

(impairment-aware RWA: IA-RWA) [47–49]. Such capability can be used as a toll for improved efficient network design and planning of advanced mesh optical networks, in the cases that long-term static as well as short-term dynamic light-path demands are considered.

The intelligence in the core optical networks should not be limited only to the network control and management planes but should also be extended to the optical layer. A key enabler to this is the use of advance impairment and performance monitoring [optical performance monitoring (OPM)] techniques, incorporated in selected optical layer network elements that can offer enhanced intelligence and enable dynamic management–compensation of the physical impairments [50]. Furthermore, as dynamic optical networks are considered more vulnerable to malfunctions and misconfigurations, OPM has a critical role to play in preventing network downtime and enabling rapid dynamic service provisioning of new connection demands while satisfying the service level agreements (SLAs) for quality of service (QoS) [51]. OPM devices will detect, identify, and locate optical degradations and provide the necessary inputs for control and management operations. Performance monitoring faces a number of challenges, namely, technological and business ones. Technology has to respond to how to cope with the increasing network complexities in real time; therefore, fast measurement acquisition is a major requirement [50,52,53]. OPM techniques should also be transparent in terms of bit rate and modulation format and provide characterization of the channel parameters, without prior knowledge of the origin and transport history of the data at arbitrary points of the network [54]. Multichannel WDM operation is also necessary and the OPM subsystems should be capable of monitoring several channels in parallel or consecutively. Increased power sensitivity is another critical issue since the OPM hardware is connected to the system via a tap coupler providing just a small amount of signal power [55]. Furthermore, the OPM techniques should provide a sufficient measurement range and resolution to accurately characterize the expected impairments [56,57]. Finally, the business challenge for OPM requires that the capital expenses should be significantly lower than the operational expenditure (OPEX) savings due to the increased reliability and the simplified operation, administration, and maintenance of the physical layer [50]. A more detailed discussion of the developed OPM technologies is presented in Subsection 4.F.

A major issue in transparent networks is the fact that failures propagate and therefore they cannot be easily localized and isolated [58]. The huge amount of information transported in optical networks requires rapid fault localization to maintain high service quality. The identification and location of failures in this type of network is a complex task mainly due to three factors: fault propagation, lack of digital penetration, and long processing times. A single failure may trigger a large number of alarms, which results in redundancy and/or false alarms for some failures. Supervisory information located in the overhead and/or payload of the data transported can only be processed at the source or destination of an optical connection, where the optical–electrical (O–E) conversions could take place. Moreover, since the problem of locating multiple faults is NP complete [59], the processing time of a fault management system of a large meshed optical network may become an issue. In distributed localization approaches, fault processing units are placed at each node of the transparent optical network. Faults are localized on the basis of local information and notification messages from neighboring nodes. We should also mention that the number of performance parameters available in the core nodes, which are fully analog, is limited. The selection of performance parameters to cover the maximum range of faults while ensuring cost-effectiveness and maintaining transparency, the placements of monitoring equipment to reduce the number of redundant alarms and to lower the capital expenses, and the design of fast localization algorithms are considered as key research topics in the field of fault diagnosis at the optical layer of transparent networks.

4. Key Enabling Technologies

In this section we present in more detail the key technologies that enable optical transparency in communication networks. For instance, we discuss switching node technologies that allow for optical bypassing and the integration of transmission and switching functionalities in the optical domain. We then discuss all-optical regeneration, FEC, and Raman amplification, which all significantly contribute to extending

the transparent length, and we review the role of novel modulation formats that enable both a reach extension and a more efficient use of the fiber's transmission bandwidth. Finally we talk about dynamically reconfigurable networks. In this respect impairment-constraint-based routing (ICBR) promises to significantly improve the blocking performance. Effective OPM techniques and efficiently designed control and management planes are required to ensure reduced reaction times and operational costs and enable more agile network behavior.

4.A. Switching Node Technologies

In wavelength routed networks transparent switching is enabled through OADMs and OXCs. These subsystems offer the capability to add and drop traffic without using optoelectronic conversions or affecting the traffic that is transmitted through the node. Thus, they can accommodate various client signals with different bit rates and formats (e.g., SONET, SDH, ATM, and IP) and forward them transparently to the end users. OADMs are used in both linear and ring network architectures, supporting one or two (bidirectional) fiber pairs, while OXCs can be used in mesh network architectures to connect a number of fiber pairs [28].

The initially proposed OADM technologies were based on passive technologies such as thin film interference filters, fiber Bragg gratings, and planar waveguides and had a fixed mode of operation. The add–drop and through channels were predetermined and could only be manually rearranged after installation. The next generation included ROADM architectures that enabled on-demand provisioning of wavelength channels without manual intervention. These architectures should ideally provide reconfigurability at a millisecond time scale, without introducing any disruption on the existing traffic during the reconfiguration process. The most common representative designs of reconfigurable OADMs are the wavelength-selective (WS) and the broadcast-and-select (B&S) architectures; see Fig. 2.

A straightforward configuration of the WS architecture, based on two cascaded WS switch (WSS) devices, is depicted in Fig. 2(a) [29]. The 1×2 WSS independently routes each of the incoming wavelength channels to one of the output ports. The 2×1 WSS selects between the through and the add ports. Other variants of this architecture also exist, i.e., using 1×2 WSS for drop and power combiners for add or power splitters for drop and 2×1 WSS for blocking and add [60]. The 1×2 WSS device, Fig. 2(a), consists of a DEMUX, which separates the wavelength channels at the ingress port, an optical switch fabric to perform the switching function, and a MUX that recombines some or all of the wavelengths to the egress port. An additional MUX can be used to connect the drop ports of the switch fabric. In general, the switch fabric of a $1\times K$ WSS device consists of several units of conventional $1\times K$ switches (one per wavelength) and K MUXs attached to them. The parameter K is used to describe the degree of the switch and it is equivalent to the potential number of network paths that may be interconnected by the device [29,61]. There are many switching technologies that enable constructing WSS elements. The most successful technology platforms are planar light-wave circuits (PLC) [30] and microelectromechanical system (MEMS) [32,62].

In the B&S architecture [see Fig. 2(b)] all incoming traffic is split into two paths for drop and pass through. In the drop part, the traffic is selected by a combination of a power splitter ($1\times N$, where N is the number of simultaneously add–drop DWDM channels at the node) and tunable filters [63,64]. This can be achieved using technologies such as acousto-optic filters (AOFs) [31] or DSEs [63] based on diffraction grating and liquid crystal or MEMS technologies that can provide simultaneous power leveling for the pass-through channels. The add path consists of N tunable transmitters and a $N\times1$ power combiner to provide the traffic. EDFAs are placed at the input and

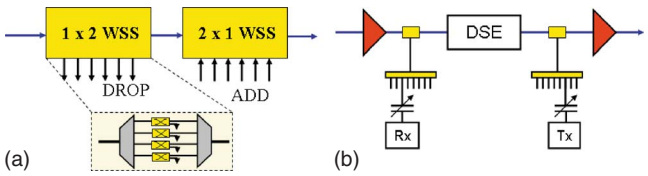

Fig. 2. (a) Wavelength-selective (WS) and (b) broadcast-and-select (B&S) OADM architectures.

the output of the OADM to compensate the corresponding losses. The enhanced flexibility of this architecture should also be noted since the tunable transmitters can emit at any slot, which is advantageous with respect to wavelength assignment and makes an efficient utilization of the available bandwidth under dynamic traffic conditions.

For mesh network topologies OXC architectures are needed to support the interconnection of different fiber pairs and to add–drop the local traffic of each node. These architectures should be scalable and provide flexible switching of any optical path without introducing disruptions to the others. Currently, most of the cross-connects that have been deployed are opaque solutions that make use of optoelectronic transceivers and an electrical core to perform switching. Each incoming wavelength is first transformed to the electrical domain, and after being switched to the appropriate port it is converted back to the optical domain. And indeed, this approach enables an efficient utilization of the available bandwidth since it may offer granularity at a subwavelength level as well as traffic grooming capabilities. On the other hand, the data rate, format, and protocol transparency are lost and the solution is not scalable to high bit rates due to the speed limitations of the electronics. The migration towards a fully transparent OXC has been achieved by replacing the electrical core of the architecture with an optical switch fabric—no longer relying on optoelectronic conversions.

For the implementation of the switching fabric various optical switching technologies have been proposed such as 2D and 3D MEMS, bubble jet, semiconductor optical amplifier (SOA) gates, holographic switches, liquid crystals, and thermo- and electro-optic switches [65]. The characteristics of these technologies are summarized in Table 1 [28].

A number of different OXC architectures have been reported in the literature [65]. The most straightforward solution is based on a central switch fabric that can potentially support a very high port count equal to [(number of fibers) × (number of wavelengths) + (number of add–drop ports)]. Based on the above formula, an OXC that supports four fiber pairs each carrying 80 wavelength channels and supporting 50% add–drop capability would require a 960×960 optical switch fabric. Beam stirring technologies such as 3D MEMS could support such a high-port-count scalable switching matrix [62]. Alternatively, a variety of multistage optical switch structures (i.e., Clos) have been proposed as well as the WS cross-connect (WSXC) architecture [66]. The latter exploits the wavelength dimension in order to conveniently segment the switching fabric, so following the wavelength demultiplexing stage the incoming wavelength channels are directed to discrete switches; see Fig. 3(a).

Another OXC architecture that provides strictly nonblocking connectivity is the B&S [Fig. 3(b)]. In this case, passive splitters and couplers combined with tunable filters are used instead of the optical switch fabric. In B&S architectures the loss of the node is significantly affected by the splitting ratio of the passive splitters that are used to broadcast and recombine the transmitted WDM signal. Therefore, they can offer low-loss OXC solutions for nodes that support a limited number of input and output fibers. This is a very attractive feature as in most practical optical network applications a small number of fibers (typically four) are interconnected at the cross-connect nodes, each carrying a large number of wavelengths (typically up to 160).

Table 1. Summary of Optical Switching Technologies

Technology	Loss (dB)	Cross Talk (dB)	PDL (dB)	Switching Time (ms)	Max Switch Dimension	Maturity
2D MEMS	5	55	0.2–0.5	<10	32×32	High
3D MEMS	7	55	0.5	<10	4000×4000	Low
Bulk mechanical	3	55	0.2	<10	16×16	High
Bubble-based waveguide	7.5	50	0.3	<10	32×32	High
Liquid crystal	1	35	0.1	<10	2×2	High
Electro-optical	8	35	0.5	<10	16×16	Low
Thermo-optical	8	35	0.5	<10	16×16	High
Holographic	1	35	Low	<10	64×64	Low
SOA	Gain	35	Low	<10	4×4	Low

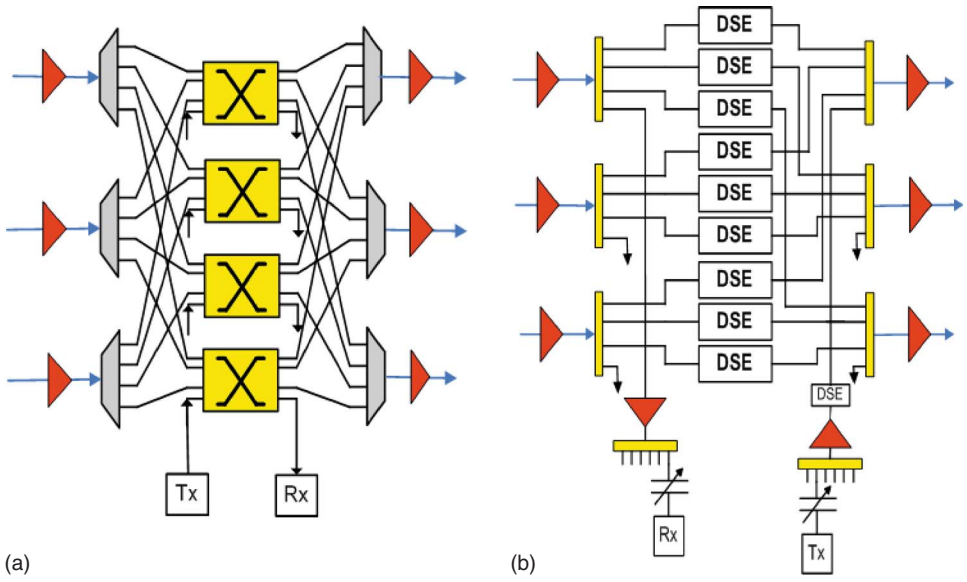

Fig. 3. OXC architectures: (a) WSXC and (b) B&S.

4.B. All-Optical Regeneration

All-optical regenerators and wavelength converters have been a topic of intense research for quite some time, and indeed, they are maturing and soon might replace power- and space-consuming OEO translator units in future transparent networks. Regenerators, either all-optical or OEO-based, are not only used to provide 2R (reamplification, reshaping) and 3R (reamplification, reshaping, and retiming) functionalities but also to take care of power equalization. Wavelength converters have also attracted much interest for use as space-switching elements in next-generation packet-switched routers. In these routers they are key elements for performing low-latency, transparent, and burst-tolerant switching [67–74]. Compared with their OEO counterparts all-optical regenerators and converters offer a number of compelling advantages:

- They hold the promise to be cheap.
- They consume little power (4 to 5 W for a 160 Gbit/s regenerator [75]).
- They need a small footprint.
- They offer bit-rate transparency within limits [67].
- They provide full protocol transparency.

State-of-the-art all-optical experiments have already demonstrated regenerative wavelength conversion at 160 [75–77] and 320 Gbits/s [78], C to L band conversion up to 640 Gbits/s [79], and all-optical demultiplexing at 320 Gbits/s [80,81] and up to 640 Gbits/s [79]. In addition to high speed they have shown ultra-long-haul 2R [82,83] and 3R capabilities [72,82,84] enabling 40 Gbit/s transmission up to 1×10^6 km [82,84]. These results have been achieved with a variety of materials, techniques, and configurations.

Among the different nonlinear materials that have been successfully used to build all optical devices for signal processing, we mainly distinguish those relying on ultrafast parametric nonlinear processes as, e.g., exploited in nonlinear fibers [85], doped glass fibers [86], holey fibers [87], or periodically poled $LiNbO_3$ materials [88], and nonparametric nonlinear material processes as, e.g., found in semiconductor materials such as lasers (DFB [89]), electroabsorption modulators (EAM) [81], or semiconductor optical amplifiers (SOAs) [77,82,90]. The former processes are ultrafast and show relaxation times below 1 ps. Also, the parameteric nonlinear effects are weak so that costly amplification of the input signals and long NL interaction lengths are quite normal (parts of meters up to several kilometers). The latter effects show relaxation times of the order of 10 ps and longer, yet the NL effects are much stronger, less optical input power is needed, and the devices typically are short (100 μm to several millimeters).

In literature, most of the regeneration and wavelength conversion implementations that have been demonstrated address on–off keying (OOK) signals. However, since

recently the trend for phase-sensitive modulation formats such as DPSK has led to the introduction of novel wavelength converter and regenerator schemes for these modulation formats. Solutions exploiting fiber nonlinearities [91,92] or FWM in SOAs have been tested [93]. Also interferometeric configurations with SOAs exploiting the more efficient SOA-based XPM effect [94–97] have demonstrated regenerative potential. SOA-based all-optical schemes have attracted attention due to the fast processing capabilities and the low power consumption and switching power requirements. On the other hand, this technology still faces technological challenges at the manufacturing level, i.e., the lack of reproducibility, which needs to be overcome in order for it to come closer to the market.

Among the different implementations for OOK signals the most common and versatile approach is based on a Mach–Zehnder interferometer (MZI) [Fig. 4(a)]. More recent interferometric approaches based on single SOA schemes have been favored due to their superior dynamic performance. The category of single SOA schemes includes the terahertz optical add–drop (TOAD) multiplexer [98,99], the ultrafast NL interferometer (UNI) [100,101], the differential delay interferometer (DI) [102,103], the redshift or blueshift optical filter (RSOF–BSOF) [90], or the pulse-reformatting optical filter (PROF) [104]. Their operational principle is the following [see Fig. 4(b)]. The input data signal P_{in} and the continuous-wave (cw) light P_{cw} are launched into the SOA. In the SOA the input data signal encodes the signal information by means of cross-gain and -phase modulation onto the cw signal. As a result we obtain at the SOA output a chirped and inverted signal P_{inv} at the wavelength of the new cw light. The purpose of the subsequent passive optical filter with an appropriate amplitude and temporal response is to reformat the signal P_{inv} into a new output-signal P_{cw} with a determined shape.

Several filters have been proposed. These are the PROF [104], the RSOF [67], and the DI [90,102,103] filter. The PROF scheme provides within first order ideal conversion efficiency [104]. It can be understood as follows. The P_{inv} signal after the SOA comprises a leading red-chirped component followed by a trailing blue-chirped component due to SOA carrier recovery and a cw tone. In the PROF scheme we suppress the cw tone and split off the red- and blue-chirped spectral components, which are subsequently recombined. This leads to a beating between the two signals that results in a strong and narrow converted pulse if the temporal delay between the two partial pulses is adapted correctly. A schematic of the filter is depicted in Fig. 5(b) and the passband of the filter around the cw frequency ν_{cw} is shown in Fig. 5(c). The RSOF scheme is similar to the PROF scheme, yet the blue-chirped components are absorbed and the redshift components form the converted signal. All other spectral parts are absorbed as indicated by the shaded area in Fig. 5(c). The absorption is at the expense of conversion efficiency. For performing fast regenerative wavelength conversion we need a differential scheme. This is provided by the DI converter scheme. In this arrangement, one either absorbs the blueshift (or redshift) components (e.g., with a waveguide grating router) and then guides the redshift (or blueshift) component into a DI. The delay and relative phase within the interferometer are chosen to interfere constructively into one output for the duration of the delay. This way we have an effective means to control the full width half-maximum. It should be noted that all the filters can be chosen to be periodic with the ITU grid and that for this reason only one filter will be needed in a WDM environment to perform multiwavelength conversion.

The strengths of the schemes have been demonstrated in recent experimental results. So, for instance, the following was shown:

- The lowest input power wavelength conversion with as little as −8.5 and −17.5 dBm signal power (measured in the fiber before the SOA) for performing

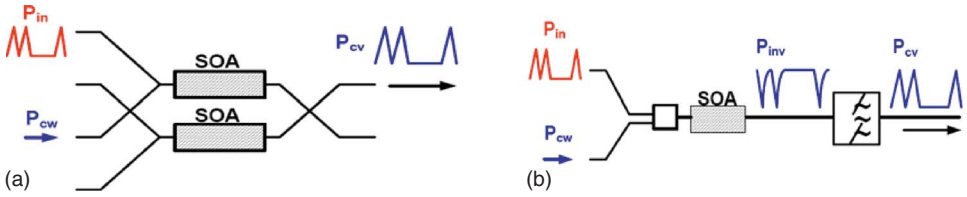

Fig. 4. (a) Conventional approach for performing all-optical wavelength conversion based on the MZI configuration. (b) Single SOA approach for performing all-optical wavelength conversion.

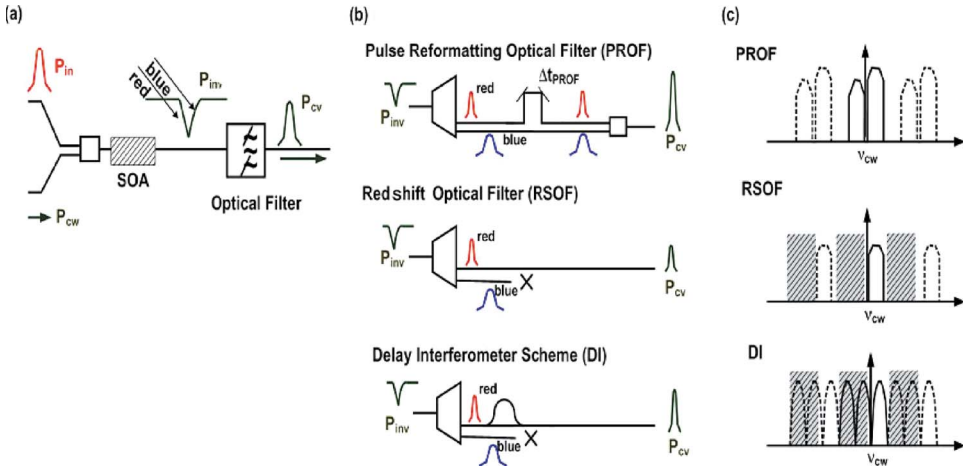

Fig. 5. (a) All-optical wavelength converter mapping an input signal P_{in} at wavelength λ_1 onto a signal P_{cw} at the new wavelength λ_2. The wavelength converter only comprises an SOA followed by an optical filter. (b) Three different optical filter concepts for performing wavelength conversion. (c) Optical spectra of the respective schemes.

40 Gbit/s return-to-zero (RZ) → RZ and RZ → NRZ wavelength conversion with a PROF scheme [104] (the input power is an order of magnitude lower than could be achieved with any previous setups) was shown. Real 2R WDM transmission over 20,000 km was demonstrated with a RSOF scheme [67].

- Successful 1×10^6 km 3R transmission was demonstrated with a DI scheme [90] and first 160 Gbit/s 3R wavelength conversion with signal regeneration. More recently, 320 Gbit/s wavelength conversion has been shown with this DI configuration [78].

Most of the all-optical regeneration techniques that have been proposed in the literature support single-channel operation. Recently, the concept of multiwavelength regeneration has appeared and is expected to provide an extremely important technological breakthrough with a significant impact in the optical communication industry in terms of system performance and the associated network economics [105,106]. One candidate technology to provide multiwavelength operation is based on the inhomogeneously broadened gain of self-assembled quantum dots in quantum dot SOAs. The spatial isolation of dots leads to spectrally localized effects and thus to cross-talk suppression between distant WDM channels. On the other hand, wavelengths with similar resonant energy levels show a strong interaction, which can be utilized for switching functions when channels are within the homogeneous broadening of the single-dot gain [107,108]. An alternative technology that has also shown similar potential is based on the phenomenon of self-phase modulation (SPM) in highly nonlinear fibers [109–111], which, in principle, can enable operation at speeds >160 Gbits/s. It is clear that multiwavelength generation has the potential to follow the paradigm of optical amplification and its application in WDM systems, which has introduced a major revolution in optical communications, making optical networking a powerful and economically viable solution.

4.C. Forward Error Correction

FEC is the most straightforward technology to overcome optical transmission limitations. FEC coding allows detection and correction of errors at the receiver side, provided the bit error rate (BER) exceeds a certain threshold, also called the FEC threshold. FEC requires a precoding of the signal, which consists of adding adequate redundant information to the signal, referred to as overhead. Borrowed from the wireless world, FEC was initially introduced in WDM optical systems to combat the ASE noise that is emitted by EDFAs. This is known as first-generation FEC technology, which was based on classic Reed–Solomon (RS) (255 239) code and provided 6 dB enhancement of OSNR sensitivity with 7% overhead. As transmission rates gradually scaled towards 10 Gbits/s, other optical impairments gained significance, such as NL effects, CD, and PMD. FEC turned out to be invaluable in mitigating these impair-

ments as well, and a second generation of FEC techniques emerged that by making use of concatenated codes and/or higher overheads achieved an additional gain of 2 dB [112].

Although a breakthrough in their own right, it was soon realized that second-generation FEC schemes do not achieve the required system margin for some important ultra-long-haul links (e.g., transpacific) [113,114]. This conclusion directed the relative research towards even stronger FEC methods. Today's state-of-the art methods, known as third-generation FEC, mostly rely on turbo and low-density parity-check (LDPC) coding concepts. They also leverage iterative decoding to obtain realizable receivers and achieve very high coding gains (CGs) in excess of 10 dB [113]. FEC methods are best characterized through BER plots that demonstrate the achievable improvement in comparison with an uncoded channel. An additive white Gaussian noise (AWGN) channel is generally used as the common reference for FEC comparisons. The performance evolution of the various generations of FEC technologies is depicted in Fig. 6.

A measure for comparison of FEC performance is the so-called CG, which expresses the equivalent increase in received power required to achieve the same BER performance increase in the absence of FEC. Traditionally, CG was measured as the horizontal distance between the BER curves of the uncoded (BER_{RAW}) and the FEC coded (BER_{FEC}) channels versus the received power, taken at a specific output BER value (usually 10^{-12}). This approach was included in the 1996 and 2000 versions of the ITU-T recommendation G.975 [116]. The CGs resulting from the above definition are rather large and counterintuitive for comparisons. Moreover, the impact of different code rates is not obvious. For these reasons, a new formula soon became the *de facto* standard for FEC performance and in 2004 was adopted by the G.975 recommendation [116]:

$$CG = 20 \log_{10}\left[\frac{\text{erfc}^{-1}(2BER_{FEC})}{\text{erfc}^{-1}(2BER_{RAW})}\right]. \quad (1)$$

Again, an AWGN channel is assumed if not otherwise stated. To take code rate (r) into account, net coding gain (NCG) is defined as

$$NCG = CG + 10 \log_{10}(r). \quad (2)$$

The above formulas facilitate comparisons between out-band and in-band FEC performance, taking the NCG of the former and the CG of the latter.

A remarkable variety of FEC systems hold a share in today's optical communications market. They differ in a number of respects, such as transmission overhead, implementation complexity, CG, BER performance, burst-error correction ability, etc. To be successful in terms of market acceptance, FEC techniques should encompass a number of important features, such as the following [115]:

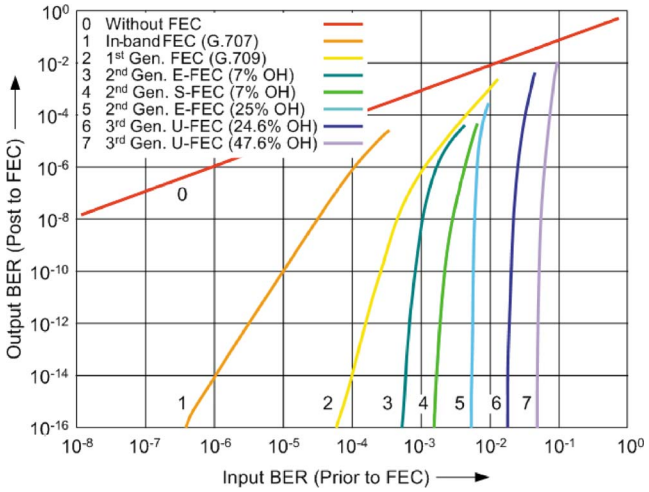

Fig. 6. FEC performance evaluation (4 and 6: experimental; 7: simulation; others: theoretical) [115].

- Processing delays. Optical communications are particularly sensitive to delays, because of the enormous traffic and the real-time requirements of many upper-layer services [e.g., voice over IP (VoIP)]. The trade-off between implementation complexity, cost, and processing delay becomes increasingly arduous, as transmission rates go higher. To obtain practical receivers, iterative decoding is of vital importance. However, the number of iterations must be carefully chosen to moderate the delays without loosing significant gain potential. Processing delays above 100 μs should be avoided.
- Rich statistics FEC. Rich statistics is the collection of additional statistical information in order to maintain the necessary system margin and to guarantee QoS. System margins are typically bound to gradually decline over time, e.g., because of the aging of components. It is therefore necessary to continually monitor the performance of optical communication links. Statistics richer than simple BER estimates are invaluable to gain further insight into the link status. Specifically, it is advisable that the error bits corrected to 0 and the bits corrected to 1 are separately counted to help identify potential sources of problems. Additionally, code words produced at the output of FEC decoders should be cross-checked and rechecked for correctness.

4.D. Raman Amplification

Since the early part of the 2000s Raman amplifiers have been deployed in long- and ultra-long-haul fiber optic transmission systems as a supplement or alternative to rare-earth-doped fibers for providing optical amplification. Their widespread acceptance is due to compelling advantages in terms of both bandwidth and transmission performance [117].

Raman amplifiers are based on the phenomenon of stimulated Raman scattering to operate. This inelastic interaction between the incident photon and molecule will cause the molecules to vibrate, resulting in the frequency downshift or the Stokes shift of the photon for the sake of energy conservation. The Raman gain depends strongly on the pump power and the frequency offset between pump and signal. Amplification occurs when the pump photon gives up its energy to create a new photon at the signal wavelength, plus some residual energy, which is absorbed as phonons (Fig. 7). The gain bandwidth is over 40 THz wide, with the dominant peak near 13.2 THz. The gain band shifts with the pump spectrum, and the peak value of the gain coefficient is inversely proportional to the pump wavelength.

A main advantage of Raman amplifiers is that a broad spectral amplification can be provided by the conventional low-loss silica fiber, i.e., the transmitting media itself. This enables a cost-effective means of upgrading from the terminal ends. Another advantage is that the gain spectrum can be tailored by the proper choice of the pump wavelength and does not depend on any wavelength-sensitive material parameter of the medium, such as the emission cross section of dopant in the Er-doped fiber. This is because the wavelength of the amplified signal is determined only by the frequency difference between the pump frequency and the frequency of the optical phonon. Based on this property one may design a Raman amplifier for ultrawideband WDM transmission using multiple pumps at different wavelengths to achieve gain flatness

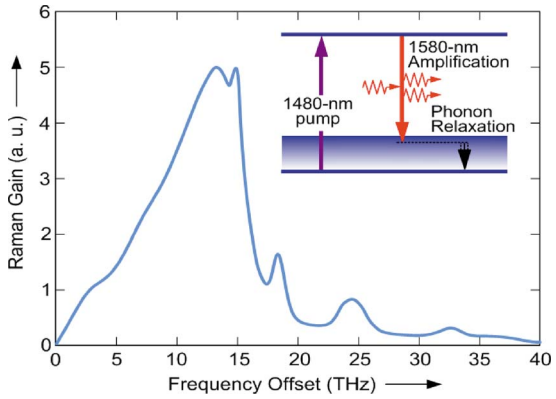

Fig. 7. Typical Raman gain efficiency spectral for single-mode fiber, and mechanism of the inelastic interaction (inset).

over an 80 nm signal bandwidth. The Raman gains created by the pumps are slightly shifted from each other so as to partly overlap forming a composite gain. We should also mention that the ASE noise in Raman amplifiers is intrinsically low, i.e., near the quantum limit of 3 dB, because the Raman amplifier is a distributed amplifier with inherently better noise figures and because of the very fast relaxation of the optical phonon, which does not allow the electrons to stay long in the lower state, and hence the inversion population is almost always complete.

Raman amplifiers can be distributed, lumped, or hybrid [118–120]. In distributed amplifiers the pump power is launched into the fiber transmission line, ensuring transmission with a reduced power level. This alleviates the influence of the nonlinear phenomena, while their effective noise figure is less than that of the EDFAs. From the aspect of system design this is translated to an increased transmission distance and the ability to support high-density WDM transmission schemes in very low dispersion regions of fibers [121]. In the lumped amplification scheme the pump power is confined within the unit of the discrete amplifier and no pump enters the transmission line. This amplification scheme offers significant advantages in terms of simplicity, cost-effectiveness, and reliability, and it is primarily used to open up new wavelength bands between 1280 and 1530 nm, a wavelength range inaccessible by EDFAs. Finally, in the hybrid scheme both distributed Raman amplifiers and EDFAs are used, complementing each other. The main advantage of the latter scheme is that it results in fewer undesirable effects due to double Rayleigh backscattering, which deteriorates the quality of the propagated signal. However the amplification bandwidth is limited by that of the EDFA.

4.E. Advanced Modulation Formats

Increased tolerance against the transmission impairments should be a main requirement for the proposed modulation schemes [39]. In particular, high resiliency to ASE noise is necessary since the optical amplifiers need to compensate losses introduced not only from the transmission fibers but also from the OADMs and OXC nodes. The RZ-DPSK format has demonstrated increased robustness against the ASE noise with more than 3 dB improvement in the OSNR sensitivity when compared to simple intensity RZ-OOK schemes [122]. DQPSK formats have also presented increased OSNR sensitivity (i.e., 1 dB improvement at 10^{-3} BER), which makes them particularly attractive in networks where spectral efficiency is highly required.

To meet the steadily growing bandwidth demands and to reduce the cost of per-bit transported information, optical networking infrastructures with high spectral efficiencies are required. Spectral efficiency, which is also referred to as information spectral density (ISD), is defined as the ratio of the individual channel bit rate to the frequency spacing (in bits/second/hertz) of the WDM channels. This quantitative measure is a conventional indicator of how closely neighboring WDM channels can be put together before their spectral overlapping will fundamentally set a limit to the ultimate capacity that can be transmitted within a given amplifier bandwidth. The next generation of 10 Gbit/s WDM transmission systems foresee a spectral efficiency of 0.4 bits/s/Hz for the NRZ intensity modulation format. Increasing the channel rate by a factor of 4 will not automatically make possible capacities greater by the same amount unless the information spectral density is increased at the same time [37]. To reach this goal, more sophisticated modulation and detection schemes are needed that do not rely exclusively on the intensity of the optical field but that also make use of its other physical attributes, such as the phase and the polarization. The recent technological advances in broadband rf electronics and optoelectronics enabled increasing complexity of the receiver–transmitter hardware and the implementation of such advanced modulations schemes at high bit rates of 40 Gbits/s.

As the optical signal traverses several nodes it experiences spectral narrowing that is introduced by the MUX–DEMUX elements along the through path. Additional bandwidth reduction effects arise from the wavelength offset that unavoidably occurs between the multiple concatenated filters or between the filters and the laser wavelength. It is highly desirable to have modulation schemes that are tolerant against this type of degradation. Traditional NRZ-OOK formats do not belong to this category because they are highly susceptible to intersymbol interference (ISI) distortions. On the other hand duobinary [123] and carrier suppressed formats [i.e., vestigial side-

band carrier-suppressed return to zero (VSB-CSRZ)] [124], as well as the RZ-DQPSK [125] have demonstrated almost no penalty in a 0.8 bit/s/Hz spectrally efficient WDM networking environment.

Dispersion issues become very critical in transparent optical networks, especially at bit rates of 40 Gbits/s and higher. In this case the time-varying character of the accumulated dispersion can significantly limit the maximum reach of the system. The dispersion variations can be attributed to temperature changes, wavelength drift in optical filters, and path reconfigurability that changes the path average dispersion [126]. An approach to overcome those limitations is found in dynamic compensation solutions. Various dynamic dispersion compensation devices based on different technologies have been proposed in recent years. These include virtually imaged phased array (VIPA) devices [127], sampled chirped fiber Bragg grating (FBG) devices [128], etalons [129,130], and planar light-wave circuits [131–134], which can be ring resonators [130], MZIs [132], and arrayed waveguide gratings (AWGs) [133,134]. CD can also be mitigated electronically through advanced signal processing techniques, implemented either at the transmitter (predistortion) or at the receiver (postcompensation). The use of electronic equalization in optical fiber communications exploits the recent advancements in high-speed digital electronics [135,136]. Two different structures have been proposed, based either on feed-forward and/or decision-feedback equalizers (FFE and/or DFE), or on maximum likelihood sequence estimation (MLSE) [137]. The first solution is comparatively simpler and has been successfully used to compensate CD- or PMD-induced degradations up 40 Gbits/s, not only for the traditional OOK scheme but also for different modulation formats [138–145]. On the other hand, the MLSE scheme is based on computationally complex Viterbi algorithms that can enable one to identify the most likely transmitted symbol sequence from the digitalized received signal. This has been a major obstacle to implementing this equalization scheme at high bit rates. To date the MLSE operation has been demonstrated only up to 10 Gbits/s [146,147]. Finally, another strategy is to use spectrally narrow schemes, such as duobinary and DQPSK, that yield significantly better dispersion tolerance. Indeed, while most of the modulation formats exhibit dispersion tolerances of the order of 50 ps/nm, duobinary and DQPSK reflect much higher values of 211 and 168 ps/nm, respectively [39,41,148].

At 40 Gbits/s a phenomenon that really worries system designers is PMD. This is caused by the imperfections in the circular symmetry of the installed fiber, which gives rise to a locally varying birefringence and results in pulse broadening and distortions depending on the signal polarization. The main problem with PMD in transmission systems is attributed to its stochastically varying nature, which is difficult to counteract. There are different solutions that could be implemented to overcome PMD limitations. One solution is to use either optical or electronic PMD compensators that would generally allow doubling the tolerance against this effect [147–158]. However, this has significant drawbacks as PMD compensators are considered expensive and complex devices that can operate only on a per-channel base. An alternative strategy could be to use a modulation format that is particularly robust to PMD. Multilevel formats such as DQPSK, which inherently use longer symbol duration are the most promising candidates since they offer approximately twice the PMD tolerance of binary modulation formats at the same bit rate.

Because of the Kerr effect, fiber nonlinearity is a main limiting factor of transparent networking. Its impact on various modulation formats depends strongly on the physical characteristics of the underlying infrastructure. At the bit rates of 2.5 or 10 Gbits/s, OOK signals are mostly limited by FWM, XPM, or SPM. Nevertheless, intrachannel nonlinearities dominate at 40 Gbits/s. A good solution for reducing transmission penalties at this bit rate is to choose modulation formats, which are more resistant to intrachannel phenomena and especially to intrachannel FWM (iFWM). A modulation format that has shown advanced performance against intrachannel degradations is CSRZ due to its alternating phases from bit-to-bit [159]. For the same reason DPSK exhibits similar resistance against intrachannel nonlinearities as CSRZ, when operated at an OSNR level that yields a BER of 10^{-3}. Nevertheless, the improved sensitivity of DPSK generally results in better BER when compared to CSRZ [160].

4.F. Routing and Wavelength Assignment

Routing in communication networks generally involves the identification of a path for each connection request. In WDM networks the wavelength of the signal should be determined. Choosing a path first and then a wavelength gives adequate results in simple topologies such as rings and trees. However, in large mesh networks significantly better results are achieved if the wavelength and route are chosen simultaneously. The resulting problem is referred to as the RWA problem.

In most RWA formulations proposed in the literature during the 1990s, the optical layer was considered as a black box and all connections were considered equally possible even though the performance for some connections might be unacceptable [161–163]. This is obviously an assumption that does not hold for several connections and especially when large core transparent networks are considered. Therefore, the routing algorithm should consider the physical limitation of the path to guarantee that the optical signal will reach the receiver with the desirable signal quality. These algorithms are reported in the literature as ICBR algorithms and ensure that connections are feasible not only relative to connectivity, capacity availability, etc., but are also relative to the physical layer performance of the connections [164–168]. The impairment constraint routing algorithms can be further improved by performing an impairment constraint wavelength assignment IA-RWA. The consideration of optimum wavelength allocation of optical signals considering physical layer limitations (i.e., by selecting portions of the spectrum with minimal impairments, increasing the wavelength spacing in these spectral regions, and giving preferential signal-to-noise-ratio treatment to these wavelengths within the optical amplifiers and switches) may enable true end-to-end transparency.

The ICBR schemes that have been proposed can be classified as static or dynamic depending on whether or not the impairments and overall network conditions are assumed to be time dependent. In the dynamic case the traffic demands and the overall network environment are assumed to vary and the physical layer parameters should be updated on a regular basis. To realize this dynamic IA-RWA option it is evident that efficient optical impairment and performance monitoring techniques are needed. The monitoring could be implemented at the impairment level [optical impairment monitoring (OIM)] or at the aggregate level where the overall performance is monitored (OPM). In the first approach, every tunable network element should report its status in terms of e.g., input–output power, noise figure, dispersion, etc. Using appropriate analytical models the effect of each physical degradation is identified. In the second approach, optical monitoring systems are located at each node for assessing the overall impact of each degradation.

A number of vendors have tried to evaluate the performance of IA-RWA algorithms [164–173]. In the heart of these activities was the development of a proprietary tool that takes into account physical layer parameters to compute a global quality factor. To incorporate the physical layer impact of a WDM network into the routing procedure there is a need to evaluate the corresponding impairments in an accurate and time efficient way. The full numerical modeling of a long-haul WDM network is computationally a very heavy procedure that might take several hours to produce a single result. On the other hand, analytical or semianalytical models for each degradation can provide an instantaneous estimation of their relative influence. For convenience all the different types of degradations should be based on a single physical layer performance metric, such as the Q-factor metric [48].

Several assumptions have been considered to achieve this. The first is that any interplay among the different types of degradations is ignored. Furthermore, noiselike distortions such as ASE, cross talk, FWM, and XPM follow Gaussian statistics. Finally, concerning the SPM, group velocity dispersion (GVD), and optical filtering effects, these are introduced through an eye closure penalty metric calculated on the most degraded bit pattern. The corresponding Q-factor penalty on the k link into the network is then given according to the following equation:

$$Q_k = \frac{pen_k P}{\sqrt{\sigma^2_{\mathrm{ASE},k} + \sigma^2_{\text{cross talk},k} + \sigma^2_{\mathrm{XPM},k} + \sigma^2_{\mathrm{FWM},k}}}, \tag{3}$$

where pen_k is the relative eye closure attributed to optical filtering and the SPM–GVD phenomena, which is calculated semianalytically through single-channel simulations according to the model proposed in [174]. Furthermore, $\sigma^2_{\mathrm{XPM},k}, \sigma^2_{\mathrm{FWM},k}$ represent the

electrical variances of the XPM- and FWM-induced degradations, which are calculated according to [175,176], and are added to the corresponding electrical variances of the ASE noise $\sigma^2_{\mathrm{ASE},k}$ and the generated crosstalk $\sigma^2_{\mathrm{cross\ talk},k}$.

A novel IA-RWA algorithm that could be utilized by a network source node to enable optimized connection provisioning and efficient resource utilization has been proposed in [177]. The flow chart of that scheme is shown in Fig. 8. Initially, the preprocessing phase collects all the information related to the network and the traffic demands. Then, based on the collected information, a Q-factor penalty is assigned [according to Eq. (3)] as a cost parameter to each link reflecting the corresponding degradations on the signal quality. The RWA phase is initiated once the link costs have been found. Incorporating the physical impairments as the weight of the links, paths, and wavelengths are assigned to all the demands. The RWA problem is handled in two steps. In the first step it is treated as a single-joint optimization problem as this has been shown to be the optimum approach. Then, the "Find k shortest paths" part of the algorithm identifies the k shortest paths for each source–destination pair. These k paths are the input for the "Do-RWA" module, which gives the algorithm the flexibility to select the optimum path among the k input paths in terms of load balancing and physical layer performance. At the end of this step the algorithm identifies the minimum number of wavelengths required to carry requests and specifies the paths that should be established. If this number is less than the wavelengths that are available in the network, then an additional blocking percentage due to lack of network resources is calculated at this stage.

Having identified the minimum number of required wavelengths along with all the established paths, the algorithm may be used to implement the specific wavelength assignment scheme. This may include either conventional strategies that are unaware of the physical performance status of the connection [such as first fit (FF) and random fit (RF)] or strategies that take into consideration the corresponding impairments. For the latter case two different schemes were examined, a direct implementation of the impairment aware wavelength assignment (IAWA), as well as a prespecified-IAWA (PS-IAWA) scheme, which for the first time to our knowledge is proposed here. In the FF scheme all wavelengths that are numbered and among those available on every link of the path, the one with the highest number is selected. In the random wavelength assignment (RF) scheme, the space of the wavelengths that are available on the required path is first identified and then one wavelength is randomly chosen. In the IAWA scheme, the light paths are established according to their Q-factor perfor-

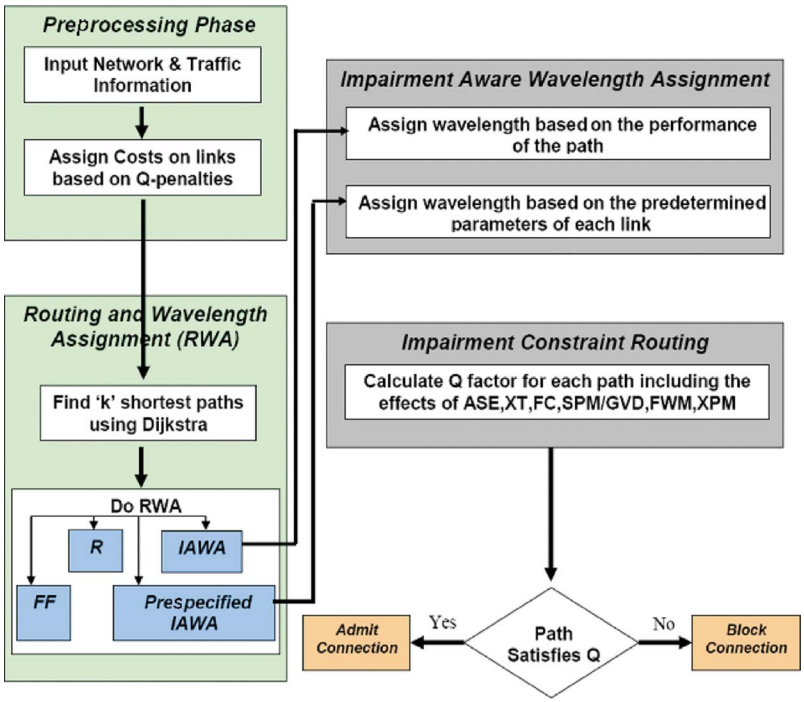

Fig. 8. Flow chart of proposed IA-RWA [177].

mance. More specifically, each potential light path, among those available on the path and taking into consideration the already established wavelength connections, is characterized in terms of Q factor. The one having the optimum performance is finally selected. The PS-IAWA scheme offers an advanced performance in terms of computational efficiency and could also be considered. According to this scheme, and prior to the wavelength assignment process, all the wavelength locations on a per-link basis are characterized and ordered in terms of their Q-factor value. Then the algorithm will define the paths and for each one of them the space of the common wavelengths that are available across its links. The final selection will be made based on the prespecified order created at the beginning.

After the wavelength assignment is completed the control is transferred to the ICBR module, which verifies the Q-factor constraint considering all the physical impairments involved across the path. In this case the overall Q factor for each selected light path is calculated considering the accumulated amount of degradation. A path is accepted when the Q-factor value at the destination node is higher than a threshold value corresponding to a BER of less than 10^{-15} after FEC is utilized and the connection is established. In any other case the path is rejected and the particular connection should be established.

4.G. Optical Monitoring and Failure Localization

OPM is considered key to self-control of next-generation networks. Advanced OPM techniques can support a number of crucial functionalities including active time-varying equalization and distortion compensation, intelligent service provisioning and traffic routing, fault forecasting, detection, diagnosis, localization and resilience mechanism activation, and signal quality characterization for QoS assurance and SLA fulfillment [178]. Different types of monitoring equipment exist in the market place and are used in transparent optical networks [179]. The majority of them work by tapping part of the optical signal using, for example, couplers. We may distinguish five different types of monitoring equipment:

- *Optical powermeter (PM)*. This monitoring equipment is able to detect any change in the power of the optical signal. It may be able to send an alarm when the measured power is different from the expected one. This equipment is very powerful for troubleshooting network faults, and since it is also very cheap it can be widely embedded in the network, especially to monitor the performance of its active elements such as EDFAs and transmitters.
- *Optical spectrum analyzer (OSA)* [180]. This equipment is able to perform analog optical signal monitoring by measuring the spectrum of the optical signal. The parameters that can be measured are channel power, channel center wavelength, and OSNR, which provides important information on the quality of the optical signal. For example, it is able to detect OSNR changes (even if they do not cause optical power variations) and the presence of unexpected out-of-band signals. The main limitation of the OSA-based noise measurements is that these assume the power levels on both sides of the channel are equal to the in-channel noise level. This assumption becomes invalid for current dense-WDM networks due to the signal overlap from neighboring channels, in-line filters, spectrum broadening from nonlinear effects, and FWM-induced noise [181,182]. On the other hand, this technique provides an excellent measure of the amplifier performance and is frequently used to locate possible EDFA failures within the network.
- *Eye monitoring*. It is able to monitor the eye diagram, which gives information on the signal distortion and can provide eye histograms by means of sampling. Sampling can be either synchronous or asynchronous. Asynchronous sampling is performed without the need for a clock recovery. Despite the simplicity of this technique, it loses in terms of accuracy and thereby has difficulties in characterizing the signal impairments. On the other hand, synchronous sampling provides higher accuracy but also is more complex and expensive. The produced histograms give information on the statistical characteristics of the optical signal with high sensitivity and form distinctive shapes that allow detection of noise, cross talk, CD, and PMD [183].
- *BER monitoring*. After converting the signal to the electrical domain, this equipment is able to calculate the BER, which is sensitive to the noise and to time distortion. This equipment is sensitive to impairments such as cross talk, CD, PMD, and optical nonlinearities; however, it is less effective at isolating the influence of the indi-

vidual impairments. BER measurements are implemented using a polling technique. Instead of terminating the optical line and having an entire bank of receivers, one per each channel, a tunable optical filter can be used that will sequentially poll each WDM channel and even multiple fibers in a single repeater. A small power percentage of 1%–2% should be tapped to guarantee that the technique is nonintrusive. BER monitoring has a low error sensitivity; therefore, it is when placed at terminal points where the performance degradation on the BER can be observed. For the cases where the BER monitor is placed at the error-free locations of the network a noise loading technique should be adopted to get an error rate at a measurable level [50].

- *rf spectrum analysis*. These techniques are based on the amplitude power spectrum and are facilitated by the use of spectral tones. This involves the generation of rf narrowband monitor signals, which are superimposed on the data signal and are used as monitoring probes. The pilot tones do not carry data but are subject to the same degradations as the signal. The tone's amplitude is a direct measure of the optical power. Additionally, the monitoring of rf tones can be used for measuring the accumulation of CD and PMD on a digital signal [184–186]. The main advantage of these techniques is that they can be implemented with narrowband electronics, which is very cost efficient. They are also applicable to a wide variety of optical modulation formats and suitable at ultra-high-speed bit rates that exceed 40 Gbits/s. Furthermore, they have high power sensitivity and fast response time (submillisecond), which makes them applicable in dynamically reconfigurable networks. Therefore, this monitoring technology could be embedded to ROADMs and OXCs and used by operators as a part of the overall network management systems.
- *Asynchronous sampling combined with pattern recognition*. This is a novel technique [187,188] that enables simultaneous monitoring of multiple impairments such as dispersion, OSNR degradation, PMD, etc. The information of the corresponding impairments is extracted through pattern recognition techniques from phase portraits that are taken by asynchronous delay-tap sampling [189]. The sample time is not related to the monitored signal bit rate, and can be many orders of magnitude slower. Furthermore, it can be used with alternative modulation formats.

Transparent networks have particularly unique features and requirements with respect to network survivability support, thus requiring a much more targeted approach in terms of network management. In particular, the peculiar behavior of transparent and all-optical components and architectures bring forth a new set of challenges for network reliability and resilience. Failure management is one of the crucial functions and a prerequisite for protection and restoration schemes. In this regard, there are many complications that prevent the continuous control and monitoring of all supported light paths simultaneously.

An important implication of using transparent components in communication systems is that available methods used to manage and monitor the health of the network may no longer be appropriate. Therefore, without additional control mechanisms, an attack upon the core network might not be detectable. In a transparent network, a light path will be capable of carrying analog and digital signals with arbitrary bit rates and protocol formats. Such a light path typically traverses multiple data links and there are many components along its route that can fail. A transmission fiber carries a number of high-bandwidth channels and its failure will cause simultaneous multiple-channel failures, resulting in large amounts of data being corrupted or compromised. Since transparent components will not by design be able to comprehend signal modulation and coding, intermediate switching nodes are unable to regenerate data, making segment-by-segment testing of communication links more demanding. As a direct consequence, failure detection and localization using existing integrity test methods are made particularly difficult.

In recent years, several studies related to the management of faults and attacks in transparent networks have been reported [190–199]. They differ on the network model that is used (e.g., a model based on the physical topology [58] or on the description of the established channels [191]), on the needed information [192] as input for the algorithm, and on the information processing methodology to locate the failures (e.g., finite state machine [193] or artificial neural networks [194]). The goal of all these methods is to identify the components whose failure has caused the received alarms. Other algorithms achieve the same goal by discarding alarms. An alarm filtering algorithm has been proposed in [196], where the considered failures are hard fail-

ures that are unexpected, such as a cut optical fiber or a broken laser. In [197] an algorithm that solves the multiple failure location problems in transparent optical networks where the failures are more deleterious and affect longer distances has been proposed. That solution also covers the nonideal scenario, where lost and/or false alarms may exist. Although the problem of locating multiple faults has been shown to be NP complete, even in the ideal scenario where no lost or false alarms exist, the proposed algorithm keeps most of its complexity in a precomputational phase. Hence, the algorithm only deals with traversing a binary tree when alarms are issued. It locates the failures based on received alarms and the failure propagation properties, which differ with the type of failure and the kind of device that exists in the network. Another algorithm has been proposed to correlate multiple security failures locally at any node and to discover their tracks through the network [195,199]. That algorithm is distributed and relies on a reliable management system since its overall success depends upon the correct message passing and processing at the local nodes. To identify the source and nature of detected performance degradation, it requires up-to-date connection and monitoring information of any established light path, on the input and output side of each node in the network. This algorithm mainly runs a generic localization procedure, which will be initiated at the downstream node that first detects serious performance degradation at an arbitrary light path on its output side. Once the origins of the detected failures have been localized, the network management system (NMS) can then make accurate decisions (for example, which offender light paths should be disconnected or rerouted) to achieve finer-grained recovery switching actions.

4.H. Control Plane and Management Issues

The role of the control plane continues to evolve as more and more intelligence is added to network elements and edge devices to control the establishment and maintenance of connections in the network. Current control plane functions include routing automatic topology and resource discovery, path computation, signaling protocols between networks switched for the establishment, maintenance, and tear-down of connections, automatic neighbor discovery, and local management to keep track of available bandwidth resources. Implementing specific control functions in the distributed control plane rather than in the centralized management plane could speed up the reaction time for most functions, increase control scalability, reduce operational time and costs, and enable more agility in the behavior of the optical network [169].

As the state of the physical network resources is constantly changing, the control and management systems, as well as the network and service operators, need to know the physical network state in order to operate correctly. Some resources and corresponding network state information is changing in a highly dynamical fashion, while other resources are more static (semistatic) and the corresponding network state information changes less frequently. Therefore the integration of physical layer impairments into the control plane is a significant task for dynamic transparent networks and feasible, cost-effective solutions must be investigated.

The Generalized Multiprotocol Label Switching (GMPLS) protocol suite, which has been developed by the Internet Engineering Task Force (IETF) [200], has gained significant momentum as a contender to become the basis of a uniform control plane that could be used for multiple network layers and be responsible for switching of packets, flows, layer 2 paths, TDM channels, wavelengths, fibers, etc. The GMPLS framework enables the capability of dynamically setting up transparent end-to-end connections but still does not offer a way of guaranteeing the end-to-end optical signal quality. A number of attempts that focus on different directions have been made to address the integration of physical layer impairments into the GMPLS control plane. The first approach deals with enhancing GMPLS signaling protocols to encompass the physical impairments. Cugini *et al.* [170] presented a novel approach by introducing the required extensions into the signaling [resource reservation protocol with traffic engineering extensions (RSVP-TE)] and management [link management protocol (LMP)] protocols. In that scheme, light-path routes from source to destination are dynamically computed by exploiting current "open shortest path first with traffic engineering extensions" (OSPF-TE) implementation, without taking into account the physical impairments. Only upon ligh-path establishment, through the reservation protocol, is the amount of impairments dynamically computed. The light-path setup request can

be either accepted or rejected based on the amount of accumulated impairments already at some intermediate node or at the destination node.

In a second approach additional information regarding the network physical parameters are inserted into the distributed routing protocol, i.e., OSPF-TE. The computation of a path request is driven by the source node of the connection by interacting with the traffic engineering database (TED), which collects the physical layer information. The TED is a repository located in each node with an updated picture of not only its local network resources (e.g., adjacent links) but also information related to remote links. Networkwide information stored in every TED serves as the input information for the RWA algorithms in order to compute optimal routes by using updated network-layer attributes. This information should be frequently updated in order to provide a high degree of accuracy and correctness to the IA-RWA algorithms implemented in the distributed control plane. For this purpose, the existent GMPLS-based routing protocols need to be extended to flood optical performance parameters as traffic engineering (TE) attributes are disseminated [171]. Impairment-related parameters are carried on the TE link state advertisements (TE-LSA).

Another direction in the integration of physical layer parameters in the control plane is the introduction of a separate component responsible for the path computation based on specified constraints. This component can be identified as an application (different building block) residing within or externally to a network node, providing optimal routes and interacting with the control plane for the establishment of the proposed paths. The path computation element (PCE) is an entity (component, application, or network node) that is capable of computing a network path or route based on a network and applying computational constraints during the computations [201]. The deployment of a dedicated PCE will relax the processing power needed by a network node to run constraint-based routing algorithms and implement highly CPU-intensive optimization techniques. Also it may eliminate the need for the network nodes to maintain the memory demanding TED by establishing it on a separate node and making it available for path computation through the PCE.

5. Conclusions

Optical transparency is widely recognized to have a central role in next-generation optical networks and to offer significant networking advancements in terms of performance and cost. The elimination of the expensive OEO equipment and the enhanced scalability of the optical technology are expected to significantly reduce the capital costs, while operational cost savings are also expected due to the faster provisioning times and the reduced power requirements. On the other hand, the actual implementation of fully transparent networks has generated new considerations and technical challenges, which might counterbalance the aforementioned benefits. To ensure the commercial and operational availability of transparency it is important to identify the benefits and limitations of today's technologies and determine what advances will be needed in order to meet the requirements of next-generation optical networks.

Real transparency can be achieved only with a combined progress in reconfigurable node architectures, robust transmission techniques, and intelligent control and management operations. Switching node technologies enabled optical bypassing, which was a major step toward the integration of transmission and switching in the optical layer. Future technical challenges include the integration of additional functionalities such as optical monitoring, dynamic allocation of the spectral bandwidth, and dynamic compensation of the physical layer impairments.

In transparent networks the physical impairments accumulate from end-to-end and can considerably affect the overall network performance. These degradations are not solely attributed to transmission phenomena but also to effects that are introduced at the switching nodes, i.e., cross talk, gain transients, etc. Novel transmission techniques are required to extend the transparent reach and achieve an efficient utilization of the fiber's transmission bandwidth. The recent achievements in FEC, Raman amplification, and modulation format technologies boosted the evolution of transparent networking, since they enabled a robust optical layer capable of serving multiterabit capacities over ultra-long-haul distances. Toward this direction we also add the recent achievements on all-optical regeneration. This technology has shown the potential to become more cost-effective and consume less power than its electronic counterparts at high bit rates.

Finally, increased intelligence is required at the optical layer to enable a more agile and resilient network performance. In particular, the integration of the physical network state into the routing decisions has promised significant operational cost benefits and has become a field of intense research over the last years. However, this has also introduced a wide variety of technical challenges, which require combined progress in the areas of both physical performance diagnosis and network control and management.

In this paper we highlighted the concept of optical transparency and discussed the challenges and the main technical breakthroughs that boosted the evolution of those networks from point-to-point links towards a high-capacity global networking platform.

References

1. A. Solheim and J. Frodsham, "Next generation backbone networks," in *Proceedings of the National Fiber Optic Engineers Conference* (2001), pp. 1283–1289.
2. I. Tomkos, M. Vasilyev, J.-K. Rhee, M. Mehendale, B. Hallock, B. Szalabofka, M. Williams, S. Tsuda, and M. Sharma, "80 × 10.7 Gb/s ultra-long-haul (+4200 km) DWDM network with reconfigurable 'Broadcast & Select' OADMs," in *Proceedings of the Optical Fiber Communication Conference* (2002), pp. FC-1-1– FC1-3.
3. Nortel Networks, "OpTera Metro 5000 Multiservice Platform," product bulletin, http://www.nortelnetworks.com/products/01/optera/metro/msp/5000/.
4. S. J. B. Yoo, "Wavelength conversion technologies for WDM network applications," J. Lightwave Technol. **14**, 955–966 (1996).
5. J. Leuthold, J. Jaques, and S. Cabot, "All-optical wavelength conversion and regeneration," in *Proceedings of the Optical Fiber Communication Conference*, Technical Digest (CD) (Optical Society of America, 2004), paper WN1.
6. R. Ramaswami, "Optical fiber communication: from transmission to networking," IEEE Commun. Mag. **40**, 138–147 (2002).
7. J. S. Cook and O. I. Szentesi, "North American field trials and early applications in telephony," IEEE J. Sel. Areas Commun. **1**, 393–397 (1983).
8. H. Ishio, "Japanese field trials and applications in telephony," IEEE J. Sel. Areas Commun. **1**, 404–412 (1983).
9. R. J. Meers, L. Reekie, M. Jauncey, and D. N. Payne, "Low noise erbium-doped fiber amplifier at 1.54 μm," Electron. Lett. **23**, 1026–1028 (1987).
10. E. Desurvire, J. R. Simpson, and P. C. Becker, "High gain erbium-doped traveling-wave fiber amplifier," Opt. Lett. **12**, 888–890 (1987).
11. T. Morioka, H. Takara, S. Kawanishi, O. Kamatani, K. Takiguchi, K. Uchiyama, M. Saruwatari, H. Takahashi, M. Yamada, T. Kanamori, and H. Ono, "100 Gb/s × 10 channel OTDM/WDM transmission using a single supercontinuum WDM source," in *Proceedings of the Optical Fiber Communication Conference* (1996), postdeadline paper PD20.
12. H. Onaka, H. Miyata, G. Ishikawa, K. Otsuka, H. Ooi, Y. Kai, S. Kinoshita, M. Seino, H. Nishimoto, and T. Chikama, "1.1 Tb/s WDM transmission over a 150 km 1.3 μm zero dispersion single mode fiber," *Optical Fiber Communication Conference*, Vol. 2 of 1996 OSA Technical Digest Series (Optical Society of America, 1996), paper PD19.
13. A. R. Chraplyvy and R. W. Tkach, "Terabit/second transmission experiments," IEEE J. Quantum Electron. **34**, 2103–2108 (1998).
14. J.-X. Cai, M. Nissov, A. N. Pilipetskii, C. R. Davidson, R.-M. Mu, M. A. Mills, L. Xu, D. Foursa, R. Menges, P. C. Corbett, D. Sutton, and N. S. Bergano, "2.4 Tb/s (120 × 20 Gb/s) transmission over transoceanic distance with optimum FEC overhead and 48 percent spectral efficiency," in *Proceedings of the Optical Fiber Communication Conference* (2001).
15. B. Bakhishi, M. F. Arend, M. Vaa, E. A. Golovchenko, D. Duff, H. Li, S. Jiang, W. W. Patterson, R. L. Maybach, and D. Kovsh, "1 Tb/s (101 × 10 Gb/s) transmission over transpacific distance using 28 nm C-band EDFAs," in *Proceedings of the Optical Fiber Communication Conference* (2001), pp. PD22/1–3.
16. G. Vareille, F. Pitel, and J. F. Marcerou, "3 Tb/s (300 × 11 Gb/s) transmission over 7380 km using 28 nm $C+L$-band with 25 GHz channel spacing and NRZ format," in *Proceedings of the Optical Fiber Communication Conference* (2001), pp. PD 24/1–3.
17. K. Fukuchi, T. Kasamatsu, M. Morie, R. Ohhira, T. Ito, K. Sekiya, D. Ogasahara, and T. Ono, "10.92-Tb/s (273 × 40 Gb/s) triple-band/ultra-dense WDM optical repeatered transmission experiment," in *Proceedings of the Optical Fiber Communication Conference* (2001), pp. PD 24/1–3.
18. S. Bigo, Y. Frignac, G. Charlet, W. Idler, S. Borne, H. Gross, R. Dischler, W. Poehlmann, P. Tran, C. Simonneau, D. Bayart, G. Veith, A. Jourdan, and J.-P. Hamaide, "10.2 Tb/s (256 × 42.7 Gb/s PDM/WDM) transmission over 100 km teralight fiber with 1.28 bit/s/Hz spectral efficiency," in *Proceedings of the Optical Fiber Communication Conference* (2001), pp. PD25/ 1–3.
19. R. E. Wagner, R. C. Alferness, A. A. M. Saleh, and M. S. Goodman, "Monet: multiwavelength optical networking," J. Lightwave Technol. **14**, 1423–1435 (1996).
20. J. Zhou, R. Cadeddu, E. Casaccia, C. Cavazzoni, and M. J. O'Mahony, "Crosstalk in multiwavelength optical cross-connect networks," J. Lightwave Technol. **14**, 1423–1435 (1996).

21. A. A. M. Saleh, "All-optical networking in metro, regional and backbone networks," in *LEOS Summer Topicals on All-Optical Networks* (2002), pp. 15.
22. J. M. Simmons, "On determining the optimal optical reach for a long-haul network," J. Lightwave Technol. **23**, 1039–1048 (2005).
23. A. F. Wallace, "Ultra long-haul DWDM: network economics," in *Proceedings of the Optical Fiber Communication Conference* (2001), paper TuT1.
24. A. Morea and J. Poirrier, "A critical analysis of the possible cost savings of translucent networks," in *5th International Workshop on Design of Reliable Communication Networks (DRCN)* (2005), pp. 311–317.
25. P. Hofmann, E. E. Basch, S. Gringeri, R. Egorov, D. A. Fishman, and W. A. Thompson, "DWDM long haul network deployment for the Verizon GNI nationwide network," in *Proceedings of the Optical Fiber Communication Conference* (2005), Vol. 2, pp. 3.
26. D. Fishman, D. L. Correa, E. H. Goode, T. L. Downs, A. Y. Ho, A. Hale, P. Hofmann, B. Basch, and S. Gringeri, "The rollout of optical networking: lambdaXtreme national network deployment," Bell Labs Technical J. **11**, 55–63 (2006).
27. D. Fishman, W. A. Thompson, and L. Vallone, "LambdaXtreme transport system: R&D of a high capacity system for low cost ultra long haul DWDM transport," Bell Labs Technical J. **11**, 27–53 (2006).
28. A. Tzanakaki, I. Zacharopoulos, and I. Tomkos, "Broadband building blocks," IEEE Circuits Devices Mag. **20**, 32–37 (2004).
29. D. T. Neilson, C. R. Doerr, D. M. Marom, R. Ryf, and M. P. Earnshaw, "Wavelength selective switching for optical bandwidth management," Bell Labs Technical J. **11**, 105–128 (2006).
30. C. R. Doerr, L. W. Stulz, D. S. Levy, L. Gomez, M. Cappuzzo, J. Bailey, R. Long, A. Wong-Foy, E. Laskowski, E. Chen, S. Patel, and T. Murphy, "Eight-wavelength add–drop filter with true reconfigurability," IEEE Photon. Technol. Lett. **15**, 138–140 (2003).
31. H. Miyata, Y. Kaito, Y. Kai, H. Onaka, T. Nakazawa, M. Doi, M. Seino, T. Chikama, Y. Kotaki, K. Wakao, M. Komiyama, T. Kunikane, H. Yonetani, and Y. Sakai, "Fully dynamic and reconfigurable optical add/drop multiplexer on 0.8 nm channel spacing using AOTF and 32-wave tunable LD module," in *Proceedings of the Optical Fiber Communication Conference* (2000), pp. 287–289.
32. J. Kim, C. J. Nuzman, B. Kumar, D. F. Lieuwen, J. S. Kraus, A. Weiss, C. P. Lichtenwalner, A. R. Papazian, R. E. Frahm, N. R. Basavanhally, D. A. Ramsey, V. A. Aksyuk, F. Pardo, M. E. Simon, V. Lifton, H. B. Chan, M. Haueis, A. Gasparyan, H. R. Shea, S. Arney, C. A. Bolle, P. R. Kolodner, R. Ryf, D. T. Neilson, and J. V. Gates, "1100×1100 port MEMS-based optical cross-connect with 4-dB maximum loss," IEEE Photon. Technol. Lett. **15**, 1537–1539 (2003).
33. I. M. Hayee and A. E. Willner, "Transmission penalties due to EDFA gain transients in add–drop multiplexed WDM networks," IEEE Photon. Technol. Lett. **11**, 889–891 (1999).
34. D. C. Kilper, S. Chandrasekhar, and C. A. White, "Transient gain dynamics of cascaded erbium-doped fiber amplifiers with re-configured channel loading," in *Proceedings of the Optical Fiber Communication Conference* (2006), Vol. 3, pp. 3.
35. A. R. Grant and D. Kilper, "Signal transient propagation in an all Raman amplified system," in *Proceedings of the Optical Fiber Communication Conference* (2004), Vol. 2, pp. 3.
36. M. Karasek and F. W. Willems, "Channel addition/removal response in cascades of strongly inverted erbium-doped fiber amplifiers," J. Lightwave Technol. **16**, 2311–2317 (1998).
37. N. Antoniades, A. Boskovic, I. Tomkos, N. Madamopoulos, M. Lee, I. Roudas, D. Pastel, M. Sharma, and M. Yadlowsky, "Performance engineering and topological design of metro WDM optical networks using computer simulations," IEEE J. Sel. Areas Commun. **20**, 149–165 (2002).
38. G. Charlet and S. Bigo, "Upgrading WDM submarine systems to 40 Gb/s channel bitrate," Proc. IEEE **94**, 935–951 (2006).
39. P. J. Winzer and R. J. Essiambre, "Advanced optical modulation formats," Proc. IEEE **94**, 952–985 (2006).
40. A. Gladisch, R.-P. Braun, D. Breuer, A. Ehrhardt, H.-M. Foisel, M. Jaeger, R. Leppla, M. Schneiders, S. Vorbeck, W. Weiershausen, and F.-J. Westphal, "Evolution of terrestrial optical system and core network architecture," Proc. IEEE **94**, 869–891 (2006).
41. J. Conradi, "Bandwidth-efficient modulation formats for digital fibre transmission systems," in *Optical Fiber Telecommunications, IV B*, I. Kaminow and T. Li, Eds. (Academic, 2002), pp. 862–901.
42. P. Peloso, M. Prunaire, L. Noirie, and D. Pennicks, "Optical transparency of a heterogeneous pan-European network," J. Lightwave Technol. **22**, 242–248 (2004).
43. B. J. Eggleton, "Dynamic dispersion, compensation devices for high speed transmission systems," in *Proceedings of the Optical Fiber Communication Conference* (2001), Vol. 3, paper WH1.
44. D. McGhan, "Electronic dispersion compensation," in *Proceedings of the Optical Fiber Communication Conference* (2006), pp. 15.
45. A. E. Willner and S. A. Havstadt, "Critical issues in reconfigurable systems and networks," *Fifth Asia-Pacific Conference on Communications and Fourth Optoelectronics and Communications Conference* (IEEE, 1999), Vol. 1, pp. 299–302.
46. C. Xie, "Performance evaluation of electronic equalizers for dynamic PMD compensation in systems with FEC," in *Proceedings of the Optical Fiber Communication Conference* (2007).
47. R. Tomkos, D. Vogiatzis, C. Mas, I. Zacharopoulos, A. Tzanakaki, and E. Varvarigos, "Performance engineering of metropolitan area optical networks through impairment constraint routing," IEEE Commun. Mag. **42**, S40–S47 (2004).
48. I. Tomkos, S. Sygletos, A. Tzanakaki, and G. Markidis, "Impairment constraint based

routing in mesh optical networks," in *Proceedings of the Optical Fiber Communication Conference* (2007), paper OWR1 (invited paper).
49. G. Markidis, S. Sygletos, A. Tzanakaki, and I. Tomkos, "Impairment constraint based routing in optical networks employing 2R regeneration," in *Proceedings of the European Conference on Optical Communications* (2006), paper Tu3.6.7.
50. D. C. Kilper, R. Bach, D. J. Blumenthal, D. Einstein, T. Landolsi, L. Ostar, M. Preis, and A. E. Willner, "Optical performance monitoring," J. Lightwave Technol. **22**, 294–304 (2004).
51. C. Pinart and G. Junyet, "The INIM system: in-service non-intrusive monitoring for QoS-enabled transparent WDM," IEEE J. Sel. Top. Quantum Electron. **12**, 635–644 (2006).
52. A. Kirstaedter, M. Wrage, G. Goeger, W. Fischler, and B. Spinnler, "Current aspects of optical performance monitoring and failure root cause analysis in optical WDM networks," Proc. SPIE **5625**, 362–373 (2005).
53. A. Richter, W. Fischler, H. Bock, R. Bach, and W. Grupp, "Optical performance monitoring in transparent and configurable DWDM networks," Proc. IEEE **149**, 1–5 (2002).
54. G. Rossi, T. E. Dimmick, and D. Blumenthal, "Optical performance monitoring in reconfigurable WDM optical networks using subcarrier multiplexing," J. Lightwave Technol. **18**, 1639–1648 (2000).
55. D. C. Kilper and W. Weingatner, "Monitoring optical network performance degradation due to amplifier noise," J. Lightwave Technol. **21**, 1171–1178 (2003).
56. S. Wielandy, M. Fishteyn, and B. Zhu, "Optical performance monitoring using nonlinear detection," J. Lightwave Technol. **22**, 784–793 (2004).
57. M. Dinu, D. C. Kilper, and H. R. Stuart, "Optical performance monitoring using data stream intensity autocorrelation," J. Lightwave Technol. **24**, 1194–1202 (2006).
58. C. Mas and P. Thiran, "An efficient algorithm for locating soft and hard failures in WDM networks," IEEE J. Sel. Areas Commun. **18**, 1900–1911 (2000).
59. N. S. V. Rao, "Computational complexity issues in operative diagnosis of graph-based systems," IEEE Trans. Comput. **42**, 447–457 (1993).
60. E. B. Basch, R. Egorov, S. Gringeri, and S. Elby, "Architectural tradeoffs for reconfigurable dense wavelength division multiplexing systems," IEEE J. Sel. Top. Quantum Electron. **12**, 615–626 (2006).
61. A. A. Saleh and J. Simmons, "Evolution towards next-generation core optical networks," J. Lightwave Technol. **24**, 3303–3321 (2006).
62. R. Ryf, J. Kim, J. P. Hickey, A. Gnauck, D. Carr, F. Pardo, C. Bolle, R. Frahm, N. Bassavanhally, C. Yoh, D. Ramsey, R. Boie, R. George, J. Kraus, C. Lichtenwalner, R. Papazian, J. Gates, H. R. Shea, A. Gasparyan, V. Muratov, J. E. Griffith, J. A. Prybyla, S. Goyal, C. D. White, M. T. Lin, R. Ruel, M. Mijander, S. Arney, D. T. Neilson, D. J. Bishop, P. Kolodner, S. Pau, C. Nuzman, A. Weis, B. Kumar, D. Lieuwen, V. Aksyuk, D. S. Greywall, T. C. Lee, H. T. Soh, W. M. Mansfield, S. Jin, W. Y. Lai, H. A. Huggins, D. L. Barr, R. A. Cirelli, G. R. Bogart, K. Teffau, R. Vella, H. Mavoori, A. Ramirez, N. A. Ciampa, F. P. Klemens, M. D. Morris, T. Boone, J. Q. Liu, J. M. Rosamilia, and C. R. Giles, "1296-port MEMS transparent optical crossconnect with 2.07 petabit/s switch capacity," in *Proceedings of the Optical Fiber Communication Conference* (2001), paper PD28.
63. M. Vasilyev, I. Tomkos, R. June-Koo Rhee, M. Mehendale, B. S. Hallock, B. K. Szalabofka, M. Williams, S. Tsuda, and M. Sharma, "Broadcast and select OADMin 80×10.7 Gb/s ultra long haul network," IEEE Photon. Technol. Lett. **15**, 332–334 (2003).
64. A. Boskovic, M. Sharma, N. Antoniades, and M. Lee, "Broadcast and select OADM nodes: application and performance trade-offs," in *Proceedings of the Optical Fiber Communication Conference* (2002), pp. 158–159.
65. H. Mouftah and J. M. H. Elmirghani, *Photon Switching Technology* (IEEE, 1999).
66. S. Mechels, L. Muller, G. D. Morley, and D. Tillett, "1D MEMS-based wavelength switching subsystem," IEEE Commun. Mag. **41**, 88–95 (2003).
67. J. Leuthold, R. Ryf, D. N. Maywar, S. Cabot, J. Jaques, and S. S. Patel, "Non-blocking all-optical cross connect based on regenerative all-optical wavelength converter in a transparent demonstration over 42 nodes and 16800 km," J. Lightwave Technol. **21**, 2863–2870 (2003).
68. D. J. Blumenthal, A. Carena, L. Rau, V. Curri, and S. Humphries, "All-optical label swapping with wavelength conversion for WDM-IP networks with subcarrier multiplexed addressing," IEEE Photon. Technol. Lett. **11**, 1497–1499 (1999).
69. S. A. Hamilton, B. S. Robinson, T. E. Murphy, S. J Savage, and E. P. Ippen, "100 Gb/s optical time-division multiplexed networks," J. Lightwave Technol. **20**, 2086–2100 (2002).
70. W. Wang, L. G. Rau, and D. J. Blumenthal, "160-Gb/s variable length packet/10-Gb/s-label all-optical label switching with wavelength conversion and unicast/multicast operation," J. Lightwave Technol. **23**, 211–218 (2005).
71. Y. Horiuchi and M. Suzuki, "Demonstration of dynamic self-routing in an all-optical burst switched mesh network with four optical label switch routers," in *Proceedings of the Optical Fiber Communication Conference* (2003), pp. 217–219.
72. J. Cao, M. Jeon, Z. Pan, Y. Bansal, Z. Wang, Z. Zhu, V. Hernandez, J. Taylor, V. Akella, and S. Yoo, "Error-free multihop cascaded operation of optical label switching routers with all-optical label swapping," in *Proceedings of the Optical Fiber Communication Conference* (2003), pp. 791–792.
73. M. Y. Jeon, Z. Pan, J. Cao, Y. Bansal, J. Taylor, Z. Wang, V. Akella, K. Okamoto, S. Kamei, J. Pan, and S. J. B. Yoo, "Demonstration of all-optical packet switching routers with optical label swapping and 2R regeneration for scalable optical label switching network applications," J. Lightwave Technol. **21**, 2723–2733 (2003).
74. D. Klonidis, R. Nejabati, C. T. Politi, M. J. O' Mahony, and D. Simeonidou, "Demonstration

of a fully functional and controlled optical packer switch at 40 Gb/s," in *Proceedings of the European Conference on Optical Communications* (2004), paper Th4.4.5.
75. J. Leuthold, L. Moller, J. Jaques, S. Cabot, L. Zhang, P. Bernasconi, M. Cappuzzo, L. Gomez, E. Laskowski, E. Chen, A. Wong-Foy, and A. Griffin, "160 Gbit/s SOA all-optical wavelength converter and assessment of its regenerative properties," Electron. Lett. **40**, 554–555 (2004).
76. C. Schubert, R. Ludwig, S. Watanabe, F. Futami, C. Schmidt, J. Berger, C. Boerner, S. Ferber, and H. G. Weber, "160 Gb/s wavelength converter with 3R-regenerating capability," Electron. Lett. **38**, 903–904 (2002).
77. S. Nakamura, Y. Ueno, and K. Tajima, "168-Gb/s all-optical wavelength conversion with a symmetric-Mach–Zehnder-type switch," IEEE Photon. Technol. Lett. **13**, 1091–1093 (2001).
78. Y. Liu, E. Tangdiongga, Z. Li, H. de Waardt, A. M. J. Koonen, G. D. Khoe, X. Shu, I. Bennion, and H. J. S. Dorren, "Error-free 320-Gb/s all-optical wavelength conversion using a single semiconductor optical amplifier," J. Lightwave Technol. **25**, 103–108 (2007).
79. H. Sotobayashi and W. Chujo, "Inter-wavelength-band conversions and demultiplexings of 640 Gb/s OTDM signals," in *Proceedings of the Optical Fiber Communication Conference* (2003), pp. 261–262.
80. S. Nakamura, Y. Ueno, and K. Tajima, "Error-free all-optical demultiplexing at 336 Gb/s with a hybrid-integrated symmetric Mach–Zehnder switch," in *Proceedings of the Optical Fiber Communication Conference* (2002), pp. FD3-1–FD3-3.
81. S. Kodama, T. Yoshimatsu, and H. Ito, "320 Gb/s optical gate monolithically integrating photodiode and electroabsorption modulator," Electron. Lett. **39**, 383–384 (2003).
82. J. Leuthold, R. Ryf, and D. Maywar, "Novel all-optical wavelength converter in an add/drop multiplexing network demonstrating transmission over 42 nodes and 16800 km," in *Proceedings of LEOS'2002 Annual Meeting* (2002), paper PD 1.3.
83. D. Rouvillain, P. Brindel, E. Sequineau, L. Pierre, O. Leclerc, H. Choumane, G. Aubin, and J. L. Oudar, "Optical 2R regenerator based on passive saturable absorber for 40 Gb/s WDM long-haul transmissions," Electron. Lett. **38**, 1113–1114 (2002).
84. G. Raybon, Y. Su, J. Leuthold, R. Essiambre, K. Dryer, T. Her, C. Jorgensen, P. Steinvurzel, and K. Feder, "40 Gb/s pseudo-linear transmission over one million kilometres," in *Proceedings of the Optical Fiber Communication Conference* (2002), pp. FD10-1–FD10-3.
85. M. Nakazawa, E. Yoshida, T. Yamamoto, E. Yamada, and A. Sahara, "TDM single channel 640 Gb/s transmission experiment over 60 km using 400 fs pulse train and walk-off free, dispersion flattened nonlinear optical loop mirror," Electron. Lett. **34**, 907–908 (1998).
86. S. Spalter, G. Lenz, R. E. Slusher, H. Y. Hwang, J. Zimmermann, T. Ktsufji, S.-W. Cheong, and M. E. Lines, "Highly nonlinear chalcogenide glasses for ultrafast all optical switching in optical TDM communication systems," in *Proceedings of the Optical Fiber Communication Conference* (2000), pp. 137–139.
87. P. Petropoulos, T. M. Monro, H. Ebendorff-Heiderpriem, K. Frampton, R. C. Moore, H. N. Rutt, and D. J. Richardson, "Soliton-self-frequency-shift effects and pulse compression in an anomalously dispersive high nonlinearity lead silicate holey fiber," in *Proceedings of the Optical Fiber Communication Conference* (2003), pp. PD3-1–3.
88. I. Brener, B. Mikkelsen, G. Raybon, R. Harel, K. Parameswaran, J. R. Kurz, and M. M. Fejer, "160 Gb/s wavelength shifting and phase conjugation using periodically poled $LiNbO_3$ waveguide parametric converter," Electron. Lett. **36**, 1788–1790 (2000).
89. M. F. C. Stephens, D. Nesset, K. A. Willians, A. E. Kelly, R. V. Penty, I. H. White, and M. J. Fice, "Wavelength conversion at 40 Gb/s via cross-gain modulation in distributed feedback laser integrated with semiconductor optical amplifier," Electron. Lett. **35**, 1762–1764 (1999).
90. J. Leuthold, G. Raybon, Y. Su, R. Essiambre, S. Cabot, J. Jaques, and M. Kauer, "40 Gbit/s transmission and cascaded all-optical wavelength conversion over 1000000 km," Electron. Lett. **38**, 890–892 (2002).
91. P. A. Andersen, T. Tokle, Y. Geng, C. Peucheret, and P. Jeppessen, "Wavelength conversion of a 40-Gb/s RZ-DPSK signal using four-wave mixing in a dispersion flattened highly nonlinear photonic crystal fiber," IEEE Photon. Technol. Lett. **17**, 1908–1910 (2005).
92. K. Croussore, C. Kim, and G. Li, "All optical regeneration of differential phase-shift keying signals based on phase-sensitive amplification," Opt. Lett. **29**, 2357–2359 (2004).
93. Z. Li, Y. Dong, J. Mo, Y. Wang, and C. Lu, "Cascaded all-optical wavelength conversion for RZ-DPSK signal based on four-wave mixing in semiconductor optical amplifier," IEEE Photon. Technol. Lett. **16**, 1685–1687 (2004).
94. V. S. Grigoryan, M. Shin, P. Devgan, J. Lasri, and P. Kumar, "SOA-based regenerative amplification of phase-noise-degraded DPSK signals: dynamic analysis and demonstration," J. Lightwave Technol. **24**, 135–142 (2006).
95. I. Kang, C. Dorrer, L. Zhang, M. Rasras, L. Buhl, A. Bhardwaj, S. Cabot, M. Dinu, X. Liu, M. Cappuzzo, L. Gomez, A. Wong-Foy, Y. F. Chen, S. Patel, D. T. Neilson, J. Jacques, and C. R. Giles, "Regenerative all-optical wavelength conversion of 40 Gb/s DPSK signals using a SOA MZI," in *Proceedings of the European Conference on Optical Communications* (2005), paper Th. 4.3.3.
96. P. Vorreau, A. Marculescu, J. Wang, G. Böttger, B. Sartorius, C. Bornholdt, J. Slovak, M. Schlak, C. Schmidt, S. Tsadka, W. Freude, and J. Leuthold, "Cascadability and regenerative properties of SOA all-optical DPSK wavelength conversion," IEEE Photon. Technol. Lett. **18**, 1970–1973 (2006).
97. A. Gnauck, "40-Gb/s RZ-differential phase shift keyed transmission," in *Proceedings of the Optical Fiber Communication Conference* (2003), pp. 450–451.

98. K. Tajima, "All-optical switch with switch-off time unrestricted by carrier lifetime," Jpn. J. Appl. Phys., Part 2 **12A**, L1746–L1749 (1993).
99. J. P. Sokoloff, P. R. Pruncal, I. Glesk, and M. Kane, "A terahertz optical asymmetric demultiplexer (TOAD)," IEEE Photon. Technol. Lett. **5**, 787–790 (1993).
100. K. Tajima, S. Sakamura, and Y. Sugimoto, "Ultrafast polarization-discriminating Mach–Zehnder all optical switch," Appl. Phys. Lett. **67**, 3709–3711 (1995).
101. K. L. Hall and K. A. Rauschenbach, "100-Gb/s bitwise logic," Opt. Lett. **23**, 1271–1273 (1998).
102. Y. Ueno, S. Nakamura, K. Tarima, and S. Kitamura, "3.8-THz wavelength conversion of picosecond pulses using a semiconductor delayed-interference signal-wavelength converter (DISC)," IEEE Photon. Technol. Lett. **10**, 346–348 (1998).
103. J. Leuthold, B. Mikkelsen, R. E. Behringer, G. Raybon, C. H. Joyner, and P. A. Besse, "Novel 3R regenerator based on semiconductor optical amplifier delayed-interference configuration," IEEE Photon. Technol. Lett. **13**, 860–862 (2001).
104. J. Leuthold, D. M. Marom, S. Cabot, J. J. Jaques, R. Ryf, and C. R. Giles, "All-optical wavelength converter based on a pulse reformatting optical filter," in *Proceedings of the Optical Fiber Communication Conference* (2003), paper PD41.
105. http://www.ihq.uni-karlsruhe.de/research/projects/TRIUMPH/.
106. I. Tomkos, A. Tzanakaki, J. Leuthold, A. D. Ellis, D. Bimberg, P. Petropoulos, D. Simeonidou, S. Tsadka, and P. Monteiro, "Transparent ring interconnection using multiwavelength photonic switches," in *International Conference on Transparent Networks* (2006), p. 23.
107. T. Akiyama, H. Kuwatsuka, T. Simoyama, Y. Nakata, K. Mukai, M. Sugawara, O. Wada, and H. Ishikawa, "Non-linear gain dynamics in quantum-dot optical amplifiers and its application to optical communication devices," IEEE J. Quantum Electron. **37**, 1059–1065 (2001).
108. M. Spyropoulou, S. Sygletos, and I. Tomkos, "Study of multi-wavelength regenerative subsystem based on quantum-dot semiconductor optical amplifiers at 40 Gbps," in *Proceedings of the Optical Fiber Communication Conference* (2007), paper JWA37.
109. M. Vasilyev and T. I. Lakoba, "All-optical multichannel 2R regeneration in a fiber-based device," Opt. Lett. **30**, 1458–1460 (2005).
110. L. A. Provost, C. Finot, P. Petropoulos, K. Mukasa, and D. Richardson, "Design scaling rules for 2R-optical self-phase modulation-based regenerators," Opt. Express **15**, 5100–5113 (2007).
111. L. Provost, Ch. Kouloumentas, F. Parmigiani, S. Tsolakidis, I. Tomkos, P. Petropoulos, and D. J. Richardson, "Experimental investigation of a dispersion-managed multi-channel 2R regenerator," *Proceedings of the Optical Fiber Communication Conference* (2008), paper OThJ3.
112. K. Seki, K. Mikami, A. Katayama, S. Suzuki, N. Shinohara, and M. Nakabayashi, "Single-chip FEC codec using a concatenated BCH code for 10 Gb/s LH optical transmission systems," in *Proceedings of the IEEE Custom Integrated Circuits Conference* (IEEE, 2003), pp. 279–282.
113. T. Mizuochi, Y. Miyata, T. Kobayashi, K. Ouchi, K. Kuno, K. Kubo, K. Shimizu, H. Taqami, H. Yoshida, H. Fujita, M. Akita, and K. Motoshima, "FEC based on block turbo code with 3 dB soft decision for 10 Gb/s optical communication systems," IEEE J. Sel. Top. Quantum Electron. **10**, 376–386 (2004).
114. T. Tsuritani, K. Ishida, A. Agata, K. Shimomura, I. Morita, T. Tokura, H. Taga, T. Mizuochi, N. Edagawa, and S. Akida, "70-GHz-spaced 42.7 GHz transpacific transmission over 9400 km using pre-filtered CSRZ-DPSK signals, all-Raman repeaters and symmetrically dispersion managed fiber spans," J. Lightwave Technol. **22**, 215–224 (2004).
115. A. Tychopoulos, O. Koufopavlou, and I. Tomkos, "A tutorial on the evolution of architectures and the future prospects of outband and inband FEC for optical communications," IEEE Circuits Devices Mag. **22**, 79–86 (2006).
116. ITU Series G: Transmission Systems and Media, Digital Systems and Networks, "Forward error correction for submarine systems," ITU-T recommendation G.975 (ITU, 1996).
117. S. Namiki, K. Seo, N. Tsukiji, and S. Shikii, "Challenges of Raman amplification," Proc. IEEE **94**, 1024–1035 (2006).
118. C. R. S. Fludger, V. Handerek, and R. J. Mears, "Ultra-wide bandwidth Raman amplifiers," in *Proceedings of the Optical Fiber Communication Conference* (2002), pp. 60–62.
119. T. Naito, T. Tanaka, K. Torii, N. Shimojoh, H. Nakamoto, and M. Suyama, "A broadband distributed Raman amplifier for bandwidths beyond 100 nm," in *Proceedings of the Optical Fiber Communication Conference* (2002), pp. 116–117.
120. L. Grüner-Nielsen, Y. Qian, B. Pàlsdóttir, P. B. Gaarde, S. Dyrbøl, and T. Verg, "Module for simultaneous C+L-band dispersion compensation and Raman amplification," in *Proceedings of the Optical Fiber Communication Conference* (2002), pp. 65–66.
121. H. Suzuki, J.-I. Kani, H. Masuda, N. Takachio, K. Iwatsuki, Y. Tada, and M. Sumida, "1-Tb/s(100×10Gb/s) super-dense WDM transmission with 25-GHz channel spacing in the zero-dispersion region employing distributed Raman amplification technology," IEEE Photon. Technol. Lett. **12**, 903–905 (2000).
122. W. A. Atia and R. S. Bondurant, "Demonstration of return-to-zero signalling in both OOK and DPSK formats to improve receiver sensitivity in an optically pre-amplified receiver," in *Proceedings of LEOS* (1999), pp. 226–227.
123. X. Zheng, F. Liu, and P. Jeppesen, "Receiver optimization for 40 Gb/s optical duobinary signal," IEEE Photon. Technol. Lett. **13**, 744–746 (2001).
124. A. H. Gnauck, P. J. Winzer, S. Chandrasekhar, and C. Dorrer, "Spectrally efficient

(0.8 b/s/Hz) 1-Tb/s (25×42.7 Gb/s) RZ-DQPSK transmission over 28 100-km SSMF spans with 7 optical add/drops," in *Proceedings of the Optical Fiber Communication Conference* (2004), paper Th4.4.1.
125. P. Mamyshev, B. Mikkelsen, F. Liu, S. Dey, J. Bennike, and C. Rasmussen, "Spectrally efficient pseudo duo-binary modulation formats for high speed optical data transmission," in *Conference on Lasers and Electro-Optics* (2002).
126. L. Shenping, M. Sauer, Z. D. Gaeta, D. V. Kuksenkov, S. R. Bickham, G. E. Berkey, L. Ming-Jun, and D. A. Nolan, "Broad-band dynamic dispersion compensation in nonlinear fiber-based device," J. Lightwave Technol. **22**, 29–38 (2004).
127. M. Shirasaki, "Chromatic-dispersion compensator using virtually angled phased array," IEEE Photon. Technol. Lett. **9**, 1598–1600 (1997).
128. Y. Painchaud, M. Lapointe, F. Trépanier, R. L. Lachance, C. Paquet, and M. Guy, "Recent progress on FBG-based tunable dispersion compensators for 40 Gb/s applications," in *Proceedings of the Optical Fiber Communication Conference* (2007), pp. 1–3.
129. T. Sugawara, S. Makio, M. Takahashi, H. Sano, M. Shishikura, and N. Kikuchi, "Low-loss 40 Gbit/s tunable dispersion compensator using highly refractive angled etalons with multiple reflections," Electron. Lett. **43**, 540–542 (2007).
130. D. J. Moss, M. Lamont, S. McLaughlin, G. Randall, P. Colbourne, S. Kiran, and C. A. Hulse, "Tunable dispersion and dispersion slope compensators for 10 Gb/s using all-pass multicavity etalons," IEEE Photon. Technol. Lett. **15**, 730–731 (2003).
131. C. K. Madsen, G. Lenz, A. J. Bruce, M. A. Cappuzzo, L. T. Gomez, and R. E. Scotti, "Integrated all-pass filters for tunable dispersion and dispersion slope compensation," IEEE Photon. Technol. Lett. **11**, 1623–1625 (1999).
132. K. Takiguchi, K. Jinguji, K. Okamoto, and Y. Ohmori, "Variable group-delay dispersion equalizer using lattice-form programmable optical filter on planar lightwave circuit," IEEE J. Sel. Top. Quantum Electron. **2**, 270–276 (1996).
133. C. R. Doerr, L. L. Buhl, M. A. Cappuzzo, E. Y. Chen, A. Wong-Foy, L. T. Gomez, R. Blum, and H. Bulthuis, "Polarization-independent tunable dispersion compensator comprised of a silica arrayed waveguide grating and a polymer slab," in *Proceedings of the Optical Fiber Communication Conference* (2006), pp. 1–3.
134. D. M. Marom, C. R. Doerr, M. A. Cappuzzo, E. Y. Chen, A. Wong-Foy, L. T. Gomez, and S. Chandrasekhar, "Compact colorless tunable dispersion compensator with 1000-ps/nm tuning range for 40-Gb/s data rates," J. Lightwave Technol. **24**, 237–241 (2006).
135. T. Nielsen and S. Chandrasekhar, "OFC 2004: workshop on optical and electronic mitigation of impairments," J. Lightwave Technol. **23**, 131–142 (2005).
136. H. Bülow, B. Franz, A. Klekamp, and F. Buchali, "40 Gb/s distortion mitigation and DSP equalization," in *Proceedings of the European Conference on Optical Communications* (2007), paper 3.3.1.
137. J. M. Gene, P. J. Winzer, S. Chandrasekhar, and H. Kogelnik, "Simultaneous compensation of polarization mode dispersion and chromatic dispersion using electronic signal processing," J. Lightwave Technol. **25**, 1735–1741 (2007).
138. H. Jiang and R. Saunders, "Advances in SiGe ICs for 40 Gb/s signal equalization," in *Proceedings of the Optical Fiber Communication Conference* (2006), paper OTuE1.
139. S. Wada, R. Ohhira, T. Ito, J. Yamazaki, Y. Amamiya, H. Takeshita, A. Noda, and K. Fukuchi, "Compensation for PMD-induced time-variant waveform distortions in 43-Gb/s NRZ transmission by ultra-wideband electrical equalizer module," in *Proceedings of the Optical Fiber Communication Conference* (2006), paper OWE2.
140. B. Franz, D. Rösener, R. Dischler, F. Buchali, B. Junginger, T. F. Meister, and K. Aufinger, "43 Gb/s SiGe based electronic equalizer for PMD and chromatic dispersion mitigation," in *Proceedings of the European Conference on Optical Communications* (2005), pp. 333–334.
141. B. Franz, A. Klekamp, D. Rösener, F. Buchali, and H. Büllow, "Performance improvements of different modulation formats by applying adaptive electronic equalization in 43 Gb/s systems," in *Proceedings of the European Conference on Optical Communications* (2007), paper 3.3.2.
142. E. Yoshida, H. Kawakami, E. Yamada, K. Kubota, Y. Miyagawa, Y. Miyamoto, T. Furuta, T. Itoh, K. Sano, and K. Murata, "Enlargement of PMD tolerance in 43 Gb/s RZ-DQPSK signal using electrical dispersion compensation without adaptive control," in *Proceedings of the European Conference on Optical Communications* (2007), paper 3.3.3.
143. A. Klekamp, B. Franz, and H. Büllow, "PMD tolerance enhancement by adaptive receiver for 43 Gb/s DPSK NRZ and RZ modulation," in *Proceedings of the European Conference on Optical Communications* (2007), paper 3.3.4.
144. C. Xie, "Performance of electronic pre-distortion in 40 Gb/s systems with optical dispersion compensation for different modulation formats and transmission fibers," in *Proceedings of the European Conference on Optical Communications* (2007), paper 3.3.5.
145. P. M. Watts, M. Glick, P. Bayvel, and R. I. Killey, "Performance of electronic pre-distortion systems with 1 sample/bit processing using optical duobinary format," in *Proceedings of the European Conference on Optical Communications* (2007), paper 3.3.6.
146. A. Färbert, "Application of digital equalization in optical transmission systems," in *Proceedings of the Optical Fiber Communication Conference* (2006), paper OTuE5.
147. A. Färbert, S. Langenbach, N. Stojanovic, C. Dorschky, T. Kupfer, C. Schulien, J.-P. Elbers, H. Wernz, H. Griesser, and C. Glingener, "Performance of a 10.7 Gb/s receiver with digital equalizer using maximum likelihood sequence estimation," in *Proceedings of the European Conference on Optical Communications* (2004), pp. 10–11.

148. S. Walklin and J. Conradi, "Multilevel signaling for increasing the reach of 10 Gb/s lightwave systems," J. Lightwave Technol. **17**, 2235–2248 (1999).
149. R. Noé, D. Sandel, M. Yoshida-Dierolf, S. Hinz, V. Mirvoda, A. Schöpflin, C. Glingener, E. Gottwald, C. Scheerer, G. Fischeer, T. Weyrauch, and W. Haase, "Polarization mode dispersion compensation at 10, 20 and 40 Gb/s with various optical equalizers," J. Lightwave Technol. **17**, 1602–1616 (1999).
150. J. C. Rasmussen, A. Isomura, and G. Ishikawa, "Automatic compensation of PMD for 40 Gb/s transmission systems," J. Lightwave Technol. **20**, 2101–2109 (2002).
151. P. C. Chou, J. M. Fini, and H. A. Haus, "Demonstration of a feed-forward PMD compensation technique," IEEE Photon. Technol. Lett. **14**, 161–163 (2002).
152. S. Bhandare and R. Noé, "Distributed PMD compensator in lithium–niobate–tantalate: performance modeling toward highest bit rates," J. Lightwave Technol. **25**, 2315–2320 (2007).
153. S. Mitani, K. Ishida, T. Sugihara, K. Shimizu, M. Takabayashi, Y. Shimakura, and K. Yoshiara, "Adaptive optical compensation with twin fiber gratings for first- and second-order PMD," in *Proceedings of the Optical Fiber Communication Conference* (2007), pp. 1–3.
154. M. Akbulut, A. M. Weiner, and P. J. Miller, "Broadband all-order polarization mode dispersion compensation using liquid-crystal modulator arrays," J. Lightwave Technol. **24**, 251–261 (2006).
155. H. F. Haunstein, W. Sauer-Greff, A. Dittrich, K. Sticht, and R. Ubransky, "Principles of electronic equilization of polarization-mode dispersion," J. Lightwave Technol. **22**, 1169–1182 (2004).
156. F. Buchali and H. Bulow, "Adaptive PMD compensation by electrical and optical techniques," J. Lightwave Technol. **22**, 1116–1126 (2004).
157. M. Jager, T. Rankl, J. Speidel, H. Bulow, and F. Buchali, "Performance of turbo equalizers for optical PMD channels," J. Lightwave Technol. **24**, 1226–1236 (2006).
158. L. L. Minkov, I. B. Djordjevic, H. G. Batshon, L. Xu, T. Wang, M. Cvijetic, and F. Kueppers, "Demonstration of PMD compensation by LDPC-coded turbo equalization and channel capacity loss characterization due to PMD and quantization," IEEE Photon. Technol. Lett. **19**, 1852–1854 (2007).
159. A. Hirano, Y. Miyamoto, K. Yonenaga, A. Sano, and H. Toba, "40 Gb/s L-band transmission experiment using SPM-tolerant carrier-suppressed RZ format," Electron. Lett. **35**, 2213–2215 (1989).
160. N. S. Bergano, "Wavelength division multiplexing in long-haul transoceanic transmission systems," J. Lightwave Technol. **23**, 4125–4139 (2005).
161. R. Mewanou and S. Pierre, "Dynamic routing algorithms in all-optical networks," in *Canadian Conference on Electrical and Computer Engineering (IEEE CCECE 2003)* (IEEE, 2003), Vol. 2, pp. 773–776.
162. D. Cavendish, A. Kolarov, and B. Sengupta, "Routing and wavelength assignment in WDM mesh networks," in *Proceedings of the Global Telecommunications Conference (GLOBECOM '04)* (IEEE, 2004), Vol. 2, pp. 1016–1022.
163. D. Banerjee and B. Mukherjee, "A practical approach for routing and wavelength assignment in large wavelength-routed optical networks," IEEE J. Sel. Areas Commun. **14**, 903–908 (1996).
164. B. Ramamurthy, D. Datta, H. Feng, J. P. Heritagen, and B. Mukherjee, "Impact of transmission impairments on the tele-traffic performance of wavelength routed optical networks," J. Lightwave Technol. **17**, 1713–1723 (1999).
165. A. Maher, D. Elie-Dit-Cosaque, and L. Tancevski, "Enhancement to multi-protocol lambda switching (MPλS) to accommodate transmission impairments," in *Proceedings of the Global Telecommunications Conference* (GLOBECOM '01) (IEEE, 2001), pp. 70–75.
166. M. Ali, D. Elie-Dit-Cosaque, and L. Tancevski, "Network optimization with transmission impairments-based routing," in *Proceedings of the European Conference on Optical Communications* (2001), pp. 42–43.
167. J. F. Martins-Filho, C. J. A. Bastos-Filho, E. A. J. Arantes, S. C. Oliveira, F. D. Nunes, R. G. Dante, and E. Fontana, "Impact of device characteristics on network performance from a physical-impairment-based routing algorithm," in *Proceedings of the Optical Fiber Communication Conference* (2006), pp. 23–27.
168. P. Kulkarni, A. Tzanakaki, C. Mas Machuka, and I. Tomkos, "Benefits of *Q*-factor based routing in WDM metro networks," in *Proceedings of the European Conference on Optical Communications* (2005), pp. 981–982.
169. R. Martinez, C. Pinart, F. Cuqini, N. Andriolli, L. Valcarenqhi, P. Castoldi, L. Wosinska, J. Cornelias, and G. Junyent, "Challenges and requirements for introducing impairment-awareness into the management and control planes of ASON/GMPLS WDM networks," IEEE Commun. Mag. **44**, 76–85 (2006).
170. F. Cugini, N. Andrioli, L. Valcarenghi, and P. Castoldi, "Physical impairment aware signaling for dynamic light-path set up," in *Proceedings of the European Conference on Optical Communications* (2005), Vol. 4, paper Th 3.5.6.
171. J. Strand, A. L. Chiu, and R. Tkach, "Issues for routing in the optical layer," IEEE Commun. Mag. **39**, 81–87 (2001).
172. G. Bogliolo, V. Curri, and M. Mellia, "Considering transmission impairments in RWA problem: greedy and metaheuristic solutions," in *Proceedings of the Optical Fiber Communication and the National Fiber Optic Engineers Conference* (IEEE, 2007), pp. 1–3.
173. Y. Huang, J. P. Heritage, and B. Makherjee, "Connection provisioning with transmission

impairment consideration in optical WDM networks with high-speed channels," J. Lightwave Technol. **23**, 982–993 (2005).
174. N. Kikuchi and S. Sasaki, "Analytical evaluation technique of self-phase modulation effect on the performance of cascaded optical amplifier systems," J. Lightwave Technol. **13**, 868–878 (1995).
175. A. Cartaxo, "Cross-phase modulation in intensity modulation direct detection WDM systems with multiple optical amplifiers and dispersion compensators," J. Lightwave Technol. **17**, 178–190 (1990).
176. K. Inoue, K. Nakanishi, and K. Oda, "Crosstalk and power penalty due to fiber four-wave mixing in multi-channel transmissions," J. Lightwave Technol. **12**, 1423–1439 (1994).
177. G. Markidis, S. Sygletos, A. Tzanakaki, and I. Tomkos, "Impairment aware based routing and wavelength assignment in transparent long haul networks," in *11th International Conference on Optical Network Design and Modeling (ONDM' 07)* (2007), pp. 48–57.
178. L.-K. Chen, M.-H. Cheung, and C.-K. Chan, "From optical performance monitoring to optical network management: research progress and challenges," in *Proceedings of the International Conference on Optical Communications and Networks (ICOCN 2004)* (2004), pp. 159–162.
179. R. Habel, K. Roberts, A. Solheim, and J. Harley, "Optical domain performance monitoring," in *Proceedings of the Optical Fiber Communication Conference* (2000), pp. 174–175.
180. S. K. Shin, K. J. Park, and Y. C. Chung, "A novel optical signal-to-noise ratio monitoring technique for WDM network," in *Proceedings of the Optical Fiber Communication Conference* (2000), pp. 182–184.
181. L. Meflah, B. Thomsen, J. Mitchell, P. Bayvel, and G. Lehmann, "Advanced optical performance monitoring for dynamically reconfigurable networks," in *Proceedings of the Conference on Networks and Optical Communication (NOC)* (2005), pp. 554.
182. D. C. Kilper, S. Chandrasekhar, L. Buhl, A. Agarwal, and D. Maywar, "Spectral monitoring of OSNR in high speed networks," in *Proceedings of the European Conference on Optical Communications* (2002), p. 7.4.4.
183. K. Mueller, N. Hanik, A. Gladisch, H.-M. Foisel, and C. Caspar, "Application of amplitude histograms for quality of service measurement of optical channels and fault identification," in *Proceedings of the European Conference on Optical Communications* (1998), pp. 707–708.
184. A. E. Willner and B. Hoanca, "Fixed and tunable management of fiber chromatic dispersion," in *Optical Fiber Telecommunications IVB*, I. Kaminov and T. Li, eds. (Academic, 2002), pp. 642–724.
185. T. Takahashi, T. Imai, and M. Aiki, "Automatic compensation technique for timewise fluctuating polarization mode dispersion in in-line amplifier systems," Electron. Lett. **30**, 348–349 (1994).
186. G. Ishikawa and H. Ooi, "Polarization-mode dispersion sensitivity and monitoring in 40-Gb/s OTDM and 10-Gb/s NRZ transmission experiments," in *Proceedings of the Optical Fiber Communication Conference* (1998), pp. 117–119.
187. T. B. Anderson, S. D. Dods, C. Clarke, J. Bedo, and A. Kowalczyk, "Multi-impairment monitoring for photonic networks (invited)," in *Proceedings of the European Conference on Optical Communications* (2007), paper 3.5.1.
188. S. D. Dods, T. B. Anderson, K. Clarke, M. Bakaul, and A. Kowalczyk, "Asynchronous sampling for optical performance monitoring," in *Proceedings of the Optical Fiber Communication Conference* (2007), pp. 1–3.
189. S. D. Dods and T. B. Anderson, "Optical performance monitoring technique using delay tap asynchronous waveform sampling," *Proceedings of the Optical Fiber Communication Conference* (2006), p. 3.
190. A. T. Bouloutas and A. Finkel, "Alarm correlation and fault identification in communication network," IEEE Trans. Commun. **42**, 523–533 (1994).
191. C. Mas, O. Crochat, and J.-Y. Le Boudec, "Fault localization for optical networks," in *Proceedings of All-Optical Networking: Architecture, Control Management Issues (SPIE'99)* (SPIE, 1998), pp. 408–419.
192. R. H. Deng, A. A. Lazar, and W. Wang, "A probabilistic approach to fault diagnosis in linear lightwave networks," IEEE J. Sel. Areas Commun. **11**, 1438–1448 (1993).
193. A. T. Bouloutas, G. W. Hart, and M. Schwartz, "Fault identification using a FSM model with unreliable partially observed data sequences," IEEE Trans. Commun. **41**, 1074–1083 (1993).
194. R. Gardner and D. Harle, "Alarm correlation and network fault resolution using Kohonen self-organizing map," in *Proceedings of the Global Telecommunications Conference (GLOBECOM'97)* (IEEE, 1997), pp. 1398–1402.
195. C. Mas and P. Thiran, "An efficient algorithm for locating soft and hard failures in WDM networks," IEEE J. Sel. Areas Commun. **18**, 1900–1911 (2000).
196. C. Mas, P. Thiran, and J.-Y. Le Boudec, "Fault location at the WDM layer," Photonic Network Commun. **1**, 235–255 (1999).
197. C. Mas, I. Tomkos, and O. K. Tonguz, "Failure location algorithm for transparent optical networks," IEEE J. Sel. Areas Commun. **23**, 1508–1519 (2005).
198. R. Rejeb, M. S. Leeson, and R. J. Green, "Cost optimization for multiple attack localization and identification in all-optical networks," in *Proceedings of the International Conference on Transparent Optical Networks (ICTON 2005)* (2005), Vol. 1, pp. 101–106.
199. R. Rejeb, M. S. Leeson, and R. J. Green, "Fault management extensions in support of GMPLS," in *Proceedings of the International Conference on Transparent Optical Networks (ICTON 2005)* (2005), Vol. 2, pp. 433–436.

200. E. Mannie, "Generalized multi-protocol label switching (GMPLS) architecture," IETF RFC 3945 (Internet Engineering Task Force, 2004).
201. A. Farrel, J-P. Vasseur, and J. Ash, "A path computation element (PCE)-based architecture," IETF RFC 4655 (Internet Engineering Task Force, 2006).